To appear in: **Mathematical Sciences**

Online ISSN: 2251-7456 Print ISSN: 2008-1359

Received: 25- September-2025

Revised: 14- February-2026

Accepted: 28- April-2026

DOI: https://doi.org/10.57647/mathsci.2026.2004.23

ORIGINAL RESEARCH

Efficient numerical solutions of proportional fractional differential equations

Lakhlifa Sadek[a,b*] Ali Algefary[c†]

[a]Department of Mathematics, Saveetha School of Engineering, Saveetha Institute of Medical and Technical Sciences, Chennai 602105, India
[b]Department of Mathematics, Faculty of Sciences and Technology, Al-Hoceima, Abdelmalek Essaadi University, Tetouan, Morocco
ORCID: 0000-0001-9780-2592.
[c]Department of Mathematics, College of Science, Qassim University, P.O. Box 6644, Buraydah 51452, Saudi Arabia
ORCID: 00009-0004-3478-7259.

Abstract

This article proposes a new family of basis functions named exp-Bernstein functions, which generalize classical Bernstein polynomials by adding an exponential term that is compatible with proportional fractional derivatives. These functions are tailored to efficiently treat generalized proportional fractional calculus operators. We propose a numerical method using exp-Bernstein functions and a collocation method for solving linear and nonlinear generalized proportional fractional Cauchy problems (GPFCPs). Our method uses an operational matrix approach to calculate proportional fractional derivatives exactly. Theoretical convergence results are also given, providing error estimates using fractional Gronwall inequalities. Numerical results show that the proposed method provides high accuracy. The exp-Bernstein basis function is particularly useful for problems with exponential kernels, which are typical of proportional fractional derivatives.

Keywords: Fractional differential equations; proportional fractional derivatives (PFD); exp-Bernstein functions; numerical analysis.

MSC 2020: 65M70, 34A08, 65D05.

1 Introduction

Fractional calculus is an extension of classical differentiation and integration to non-integer orders [1]. Among different fractional operators, proportional fractional derivatives have attracted interest owing to the combination of exponential kernels and fractional differentiation [2–4]. These fractional derivatives have been used in modeling viscoelasticity, anomalous transport, control theory, and biological systems [5–8].

*Email: l.sadek@uae.ac.ma
†Corresponding author: a.algefary@qu.edu.sa

The numerical solution of Fractional Differential Equations (FDEs) using orthogonal polynomials (Legendre, Chebyshev, Jacobi) [9–11], wavelet bases [12,13], quadratic function preserving wavelet type Baskakov operators [14] or Müntz polynomials [15–17], Korovkin's type approximation [18] and Sadek and Sami Bataineh in [19] give general of Bernstein polynomial for solving FDE with fractional operators respect to another function. However, these methods need to be modified for proportional fractional derivatives, which have an exponential kernel

The construction of efficient numerical schemes for solving fractional differential equations has been an active research field, with different methods being proposed to tackle the special difficulties. Recent years have witnessed the use of a broad range of methods, including meshless methods and barycentric rational interpolation for stochastic fractional integro-differential equations [23–25], which indicate the demand for efficient and reliable numerical methods. Finite element and finite difference methods have also been widely investigated for solving multi-dimensional fractional problems [26]. In the framework of polynomial-based methods, fractional-order orthogonal polynomials, such as Bernstein polynomials, have been successfully used for solving nonlinear fractional Volterra integro-differential equations and matrix equations [27–29] and Chebyshev in [30]. Moreover, the generalized Taylor collocation methods have been applied to the classical fractional equations, such as the Bagley-Torvik equation [31]. Although these methods are very useful, they are mostly developed for Riemann-Liouville or Caputo fractional operators and may need considerable adjustments or have errors in numerical quadratures when applied to proportional fractional derivatives, which have a specific exponential kernel. The purpose of this study is to fill this particular gap by proposing exp-Bernstein functions, which have a basis set naturally aligned with this kernel, providing a more natural and efficient approach compared to the existing ones.

Main contributions

This work makes the following key contributions:

- Introduction of exp-Bernstein functions: exponential extensions of Bernstein polynomials compatible with PFD.
- Derivation of an exact operational matrix for PFD applied to exp-Bernstein bases.
- Development of a collocation method for GPFCPs.
- Rigorous convergence analysis using fractional Gronwall inequalities.
- Comprehensive numerical validation demonstrating superior accuracy compared to existing methods.

Problem formulation

We consider the GPFCP:

$$ {}^{C}D^{\alpha,\gamma}_{a,\Theta} y(\Theta) = g(\Theta, y(\Theta)), \quad a \le \Theta \le b, \quad \alpha \in (0,1], \tag{1} $$

with initial condition

$$ y(a) = y_a, \tag{2} $$

where ${}^{C}D^{\alpha,\gamma}_{a,\Theta}$ denotes the left Caputo proportional fractional derivative of order α with proportionality parameter $\gamma \in (0,1]$.

Section 2 reviews fractional calculus fundamentals. Section 3 defines exp-Bernstein functions and their properties. Section 4 discusses function approximation. Section 5 the proportional fractional derivative of the exp-Bernstein basis vector. Section 6 presents the numerical scheme. Section 7 provides convergence analysis. Section 8 shows numerical experiments. Section 9 concludes with future directions.

2 Preliminaries and mathematical background

Definition 1. *[1] For $\alpha \in (0,1]$, the left-sided Riemann-Liouville fractional integral is*

$$I^{\alpha}_{a,\Theta} y(\Theta) = \frac{1}{\Gamma(\alpha)} \int_a^{\Theta} (\Theta - s)^{\alpha-1} y(s) ds, \tag{3}$$

where $\Gamma(\cdot)$ is the Euler gamma function.

Definition 2. *[1] For $\alpha \in (0,1]$, the left-sided Caputo fractional derivative is*

$${}^{C}D^{\alpha}_{a,\Theta} y(\Theta) = \frac{1}{\Gamma(1-\alpha)} \int_a^{\Theta} (\Theta - s)^{-\alpha} \dot{y}(s) ds. \tag{4}$$

Definition 3. *[2] Let $\alpha \in (0,1]$ and $\gamma \in (0,1]$. The left proportional fractional integral is*

$${}_{a}I^{\alpha,\gamma}_{\Theta} y(\Theta) = \frac{1}{\gamma^{\alpha}\Gamma(\alpha)} \int_a^{\Theta} e^{\frac{\gamma-1}{\gamma}(\Theta-s)} (\Theta - s)^{\alpha-1} y(s) ds, \tag{5}$$

and the left proportional fractional derivative is

$${}^{C}_{a}D^{\alpha,\gamma}_{\Theta} y(\Theta) = \frac{\gamma^{\alpha-1}}{\Gamma(1-\alpha)} \int_a^{\Theta} \frac{e^{\frac{\gamma-1}{\gamma}(\Theta-s)}}{(\Theta - s)^{\alpha}} (D^{1,\gamma} y)(s) ds, \tag{6}$$

where $(D^{1,\gamma} y)(s) = (1-\gamma) y(s) + \gamma \dot{y}(s)$.

Proposition 1. *[2] Let $\gamma \in (0,1]$, $\alpha \in (0,1]$, and $\eta > 0$. Let $f(\Theta) = e^{\frac{\gamma-1}{\gamma}(\Theta-a)} (\Theta - a)^{\eta}$. Then*

1.

$${}_{a}I^{\alpha,\gamma}_{\Theta} f(\Theta) = \frac{\Gamma(\eta+1)}{\gamma^{\alpha}\Gamma(\eta+1+\alpha)} e^{\frac{\gamma-1}{\gamma}(\Theta-a)} (\Theta - a)^{\eta+\alpha}. \tag{7}$$

2.

$${}^{C}_{a}D^{\alpha,\gamma}_{\Theta} f(\Theta) = \frac{\gamma^{\alpha}\Gamma(\eta+1)}{\Gamma(\eta+1-\alpha)} e^{\frac{\gamma-1}{\gamma}(\Theta-a)} (\Theta - a)^{\eta-\alpha}. \tag{8}$$

3.

$${}^{C}_{a}D^{\alpha,\gamma} e^{\frac{\gamma-1}{\gamma}(\Theta-a)} = 0. \tag{9}$$

Theorem 1. *[2] Let $\gamma \in (0,1]$ and $\alpha \in (0,1]$. Then*

$${}_{a}I^{\alpha,\gamma}_{\Theta} \left({}^{C}_{a}D^{\alpha,\gamma}_{\Theta} y \right)(\Theta) = y(\Theta) - y(a) e^{\frac{\gamma-1}{\gamma}(\Theta-a)}.$$

Lemma 1. *[32] Let $\alpha, \gamma \in (0,1]$, $u(\Theta), v(\Theta)$ be nonnegative functions locally integrable on $[a,b)$ and $w \geq 0$. If*

$$u(\Theta) \leq v(\Theta) + \gamma^{\alpha}\Gamma(\alpha) w \left({}_{a}I^{\alpha,\gamma}_{\Theta} u \right)(\Theta),$$

then

$$u(\Theta) \leq v(\Theta) \mathbb{E}_{\alpha}(w\Gamma(\alpha), \Theta), \quad \Theta \in [a,b),$$

where $\mathbb{E}_{\alpha}(\lambda, z) = \sum_{k=0}^{\infty} \frac{\lambda^k z^{k\alpha}}{\Gamma(\alpha k+1)}$ is the one-parameter Mittag-Leffler function.

Definition 4. *[28] Let $m \in \mathbb{N}$. The Bernstein polynomials on $[a, b]$ are*

$$B_l^m(\Theta) = \frac{\binom{m}{l}}{(b-a)^m}(\Theta - a)^l (b - \Theta)^{m-l}, \quad l = 0, \ldots, m. \tag{10}$$

3 Exponential-Bernstein functions

3.1 Definition and basic properties

Definition 5. *For $m \in \mathbb{N}$ and $\gamma \in (0, 1]$, the exp-Bernstein functions of degree m are defined as*

$${}^{\gamma}EB_l^m(\Theta) = e^{\frac{\gamma-1}{\gamma}(\Theta-a)} \frac{\binom{m}{l}}{(b-a)^m}(\Theta - a)^l (b - \Theta)^{m-l}, \quad l = 0, \ldots, m. \tag{11}$$

Remark 1. *For $\gamma = 1$, the exp-Bernstein functions reduce to classical Bernstein polynomials: ${}^{1}EB_l^m(\Theta) = B_l^m(\Theta)$.*

Figure 1 illustrates the exp-Bernstein basis functions used for blending a third-degree curve.

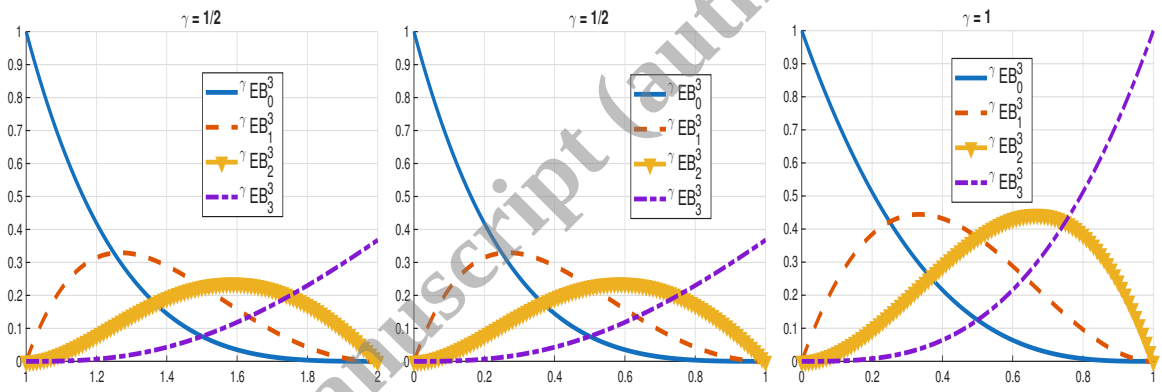

Figure 1: Curve blending of degree three using exp-Bernstein basis functions.

Lemma 2. *For $m, k \in \mathbb{N}$ and exp-Bernstein functions ${}^{\gamma}EB_k^m(\Theta)$, we have*

$${}^{\gamma}EB_l^m(\Theta) = \sum_{j=0}^{m-l} (-1)^j \binom{m}{l} \binom{m-l}{j} e^{\frac{\gamma-1}{\gamma}(\Theta-a)} \left(\frac{\Theta - a}{b-a}\right)^{l+j}. \tag{12}$$

Proof. Using the binomial expansion $(1-z)^{m-l} = \sum_{j=0}^{m-l} (-1)^j \binom{m-l}{j} z^j$, we obtain

$$\begin{aligned}
{}^{\gamma}EB_l^m(\Theta) &= \binom{m}{l} \left(\frac{\Theta - a}{b-a}\right)^l \left(1 - \frac{\Theta - a}{b-a}\right)^{m-l} e^{\frac{\gamma-1}{\gamma}(\Theta-a)} \\
&= \binom{m}{l} \left(\frac{\Theta - a}{b-a}\right)^l \sum_{j=0}^{m-l} (-1)^j \binom{m-l}{j} \left(\frac{\Theta - a}{b-a}\right)^j e^{\frac{\gamma-1}{\gamma}(\Theta-a)} \\
&= \sum_{j=0}^{m-l} (-1)^j \binom{m}{l} \binom{m-l}{j} e^{\frac{\gamma-1}{\gamma}(\Theta-a)} \left(\frac{\Theta - a}{b-a}\right)^{l+j}.
\end{aligned}$$

□

3.2 Matrix representation

Define the weight matrix $\mathbb{W}_{l+1} \in \mathbb{R}^{1\times(m+1)}$

$$\mathbb{W}_{l+1} := \left[0,\ldots,0,\frac{(-1)^0}{h^l}\binom{m}{l},\frac{(-1)^1}{h^{l+1}}\binom{m}{l}\binom{m-l}{1},\ldots,\frac{(-1)^{m-l}}{h^m}\binom{m}{l}\binom{m-l}{m-l}\right], \quad (13)$$

where $h = b - a$. Then from Lemma 2, we have

$$^{\gamma}EB_l^m(\Theta) = \mathbb{W}_{l+1}\mathbb{V}_m(\Theta), \quad (14)$$

with

$$\mathbb{V}_m(\Theta) = \left[e^{\frac{\gamma-1}{\gamma}(\Theta-a)}, e^{\frac{\gamma-1}{\gamma}(\Theta-a)}(\Theta-a),\ldots,e^{\frac{\gamma-1}{\gamma}(\Theta-a)}(\Theta-a)^m\right]^T. \quad (15)$$

Let $\mathbb{U} = [\mathbb{W}_1^T, \mathbb{W}_2^T, \ldots, \mathbb{W}_{m+1}^T]^T \in \mathbb{R}^{(m+1)\times(m+1)}$. Then

$$\Psi(\Theta) = \mathbb{U}\mathbb{V}_m(\Theta), \quad (16)$$

where $\Psi(\Theta) = [^{\gamma}EB_0^m(\Theta), ^{\gamma}EB_1^m(\Theta), \ldots, ^{\gamma}EB_m^m(\Theta)]^T$. Comparison with classical Bernstein basis in Table 1.

Table 1: Comparison between classical Bernstein and exp-Bernstein functions

Classical Bernstein Polynomials	exp-Bernstein Functions
Definition: $B_l^m(\Theta) = \binom{m}{l}(\Theta-a)^l(b-\Theta)^{m-l}/(b-a)^m$,	Definition: $^{\gamma}EB_l^m(\Theta) = e^{\frac{\gamma-1}{\gamma}(\Theta-a)}B_l^m(\Theta)$,
Kernel Compatibility: Incompatible with exponential kernel	Kernel Compatibility: Built-in exponential term matches proportional derivative kernel
Fractional Derivative: Difficult to compute exactly	Fractional Derivative: Can be computed exactly via operational matrix
Special Case: General polynomial basis	Special Case: Reduces to Bernstein when $\gamma = 1$

4 Function aproximation with exp-Bernstein basis

Let $H = L^2([a,b])$ and $^{\gamma}Y = \text{span}\{^{\gamma}EB_0^m, ^{\gamma}EB_1^m, \ldots, ^{\gamma}EB_m^m\} \subset H$.

Theorem 2. *Let $h \in H$, there exists a unique $h_0 \in {}^{\gamma}Y$ such that*

$$\|h - h_0\|_{L^2([a,b])} \leq \|h - g\|_{L^2([a,b])}, \quad \forall g \in {}^{\gamma}Y. \quad (17)$$

Proof. The set $\{\gamma EB_0^m, \gamma EB_1^m, \ldots, \gamma EB_m^m\}$ consists of $m+1$ linearly independent functions. Hence, γY is a finite-dimensional subspace of H. In a Hilbert space, every finite-dimensional

subspace is closed. Therefore, γY is closed. Since H is a Hilbert space and γY is a closed subspace, by the projection Theorem, for any $h \in H$, there exists a unique $h_0 \in \gamma Y$ such that

$$\|h - h_0\| = \inf_{g \in \gamma Y} \|h - g\|.$$

This h_0 is the orthogonal projection of h onto γY. By definition of the infimum and the uniqueness of h_0, we have

$$\|h - h_0\| \leq \|h - g\|, \quad \forall g \in \gamma Y.$$

The best approximation h_0 satisfies the orthogonality condition

$$\langle h - h_0, g \rangle = 0, \quad \forall g \in \gamma Y.$$

Thus, there exists a unique $h_0 \in \gamma Y$ that minimizes the distance from h in the L^2-norm, completing the proof. □

Theorem 3. *Any $h \in L^2([a,b])$ can be approximated as*

$$h(\Theta) \approx h_0(\Theta) = \sum_{j=0}^{m} c_j {}^{\gamma}EB_j^m(\Theta) = C\Psi(\Theta), \tag{18}$$

where $C = [c_0, c_1, \ldots, c_m]$ and the coefficients satisfy

$$RC^T = K, \quad \text{with } R_{ji} = \langle {}^{\gamma}EB_j^m, {}^{\gamma}EB_i^m \rangle, \quad K_i = \langle h, {}^{\gamma}EB_i^m \rangle. \tag{19}$$

Thus $C = K^T R^{-1}$.

Proof. Since ${}^{\gamma}Y = \text{span}\{{}^{\gamma}EB_0^m, {}^{\gamma}EB_1^m, \ldots, {}^{\gamma}EB_m^m\}$ is a finite-dimensional subspace of the Hilbert space $H = L^2([a,b])$, it is closed. By the projection theorem for Hilbert spaces, for any $h \in H$, there exists a unique best approximation $h_0 \in {}^{\gamma}Y$ that minimizes the distance

$$\|h - h_0\|_{L^2([a,b])} = \min_{g \in \gamma Y} \|h - g\|_{L^2([a,b])}.$$

The best approximation h_0 is characterized by the orthogonality condition

$$\langle h - h_0, g \rangle = 0 \quad \text{for all } g \in {}^{\gamma}Y.$$

In particular, this holds for each basis function ${}^{\gamma}EB_i^m$, $i = 0, 1, \ldots, m$ is

$$\langle h - h_0, {}^{\gamma}EB_i^m \rangle = 0, \quad i = 0, 1, \ldots, m. \tag{20}$$

Since $h_0 \in {}^{\gamma}Y$, it can be expressed as a linear combination of the basis functions

$$h_0(\Theta) = \sum_{j=0}^{m} c_j {}^{\gamma}EB_j^m(\Theta),$$

or in vector form $h_0(\Theta) = C\Psi(\Theta)$ where $C = [c_0, c_1, \ldots, c_m]$ and

$$\Psi(\Theta) = [{}^{\gamma}EB_0^m(\Theta), {}^{\gamma}EB_1^m(\Theta), \ldots, {}^{\gamma}EB_m^m(\Theta)]^T.$$

Substituting the expression for h_0 into the orthogonality condition (20), we have

$$\left\langle h - \sum_{j=0}^{m} c_j {}^{\gamma}EB_j^m, {}^{\gamma}EB_i^m \right\rangle = 0, \quad i = 0, 1, \ldots, m.$$

Using linearity of the inner product

$$\langle h, {}^{\gamma}EB_i^m\rangle - \sum_{j=0}^{m} c_j \langle {}^{\gamma}EB_j^m, {}^{\gamma}EB_i^m\rangle = 0, \quad i = 0, 1, \ldots, m.$$

Rearranging

$$\sum_{j=0}^{m} c_j \langle {}^{\gamma}EB_j^m, {}^{\gamma}EB_i^m\rangle = \langle h, {}^{\gamma}EB_i^m\rangle, \quad i = 0, 1, \ldots, m. \tag{21}$$

Define the Gram matrix R and vector K as

$$R_{ji} = \langle {}^{\gamma}EB_j^m, {}^{\gamma}EB_i^m\rangle, \quad K_i = \langle h, {}^{\gamma}EB_i^m\rangle.$$

Note that R is symmetric since $R_{ji} = \langle {}^{\gamma}EB_j^m, {}^{\gamma}EB_i^m\rangle = \langle {}^{\gamma}EB_i^m, {}^{\gamma}EB_j^m\rangle = R_{ij}$. The system (21) can be written in matrix form as

$$\begin{bmatrix} R_{00} & R_{01} & \cdots & R_{0m} \\ R_{10} & R_{11} & \cdots & R_{1m} \\ \vdots & \vdots & \ddots & \vdots \\ R_{m0} & R_{m1} & \cdots & R_{mm} \end{bmatrix} \begin{bmatrix} c_0 \\ c_1 \\ \vdots \\ c_m \end{bmatrix} = \begin{bmatrix} K_0 \\ K_1 \\ \vdots \\ K_m \end{bmatrix}.$$

In compact notation

$$RC^T = K. \tag{22}$$

To show that R is invertible, we prove that it is positive definite. For any non-zero vector $\mathbf{v} = [v_0, v_1, \ldots, v_m]^T \in \mathbb{R}^{m+1}$, consider

$$\mathbf{v}^T R \mathbf{v} = \sum_{i=0}^{m}\sum_{j=0}^{m} v_i v_j R_{ij} = \sum_{i=0}^{m}\sum_{j=0}^{m} v_i v_j \langle {}^{\gamma}EB_i^m, {}^{\gamma}EB_j^m\rangle.$$

By linearity

$$\mathbf{v}^T R \mathbf{v} = \left\langle \sum_{i=0}^{m} v_i {}^{\gamma}EB_i^m, \sum_{j=0}^{m} v_j {}^{\gamma}EB_j^m \right\rangle = \left\| \sum_{i=0}^{m} v_i {}^{\gamma}EB_i^m \right\|^2_{L^2([a,b])}.$$

Since the exp-Bernstein functions $\{{}^{\gamma}EB_i^m\}_{i=0}^m$ are linearly independent, $\sum_{i=0}^m v_i {}^{\gamma}EB_i^m \neq 0$ for $\mathbf{v} \neq 0$. Therefore

$$\mathbf{v}^T R \mathbf{v} = \left\| \sum_{i=0}^{m} v_i {}^{\gamma}EB_i^m \right\|^2 > 0 \quad \text{for all } \mathbf{v} \neq 0.$$

Thus R is positive definite, hence invertible. Since R is invertible, we can solve (22) for C^T:

$$C^T = R^{-1}K \quad \Rightarrow \quad C = (R^{-1}K)^T = K^T R^{-1}.$$

The last equality uses the symmetry of R (and hence of R^{-1}). The approximation error is given by

$$\|h - h_0\|^2_{L^2([a,b])} = \|h\|^2 - \|h_0\|^2,$$

which follows from the orthogonality condition. Since h_0 is the best approximation in ${}^{\gamma}Y$, this error is minimized among all approximations in the subspace. In practice, the inner products can be computed as

$$\langle {}^{\gamma}EB_j^m, {}^{\gamma}EB_i^m\rangle = \int_a^b {}^{\gamma}EB_j^m(\Theta) {}^{\gamma}EB_i^m(\Theta)\, d\Theta,$$

$$\langle h, {}^{\gamma}EB_i^m \rangle = \int_a^b h(\Theta)\, {}^{\gamma}EB_i^m(\Theta)\, d\Theta.$$

□

Remark 2. *The Gram matrix R is not only symmetric and positive definite, but also typically well-conditioned for the exp-Bernstein basis, especially for moderate values of m. This ensures numerical stability when solving for the coefficients.*

Remark 3. *For $\gamma = 1$, the exp-Bernstein functions reduce to classical Bernstein polynomials, and the approximation formula becomes the standard Bernstein approximation. In this case, the Gram matrix R can be computed analytically using properties of Beta functions.*

Corollary 1. *As $m \to \infty$, the approximation h_0 converges to h in the L^2 norm*

$$\lim_{m\to\infty} \|h - h_0\|_{L^2([a,b])} = 0.$$

As m increases, the approximation space becomes richer, leading to improved accuracy.

5 The proportional fractional derivative of the exp-Bernstein basis vector

Theorem 4. *The proportional fractional derivative of the exp-Bernstein basis vector satisfies*

$${}^{C}D_{a,\Theta}^{\alpha,\gamma}\Psi(\Theta) = \mathbb{U}\Omega\mathbb{Z}(\Theta), \tag{23}$$

where

$$\Omega = diag\left(0, \frac{\gamma^{\alpha}\Gamma(2)}{\Gamma(2-\alpha)}, \frac{\gamma^{\alpha}\Gamma(3)}{\Gamma(3-\alpha)}, \ldots, \frac{\gamma^{\alpha}\Gamma(m+1)}{\Gamma(m+1-\alpha)}\right),$$

and $\mathbb{Z}(\Theta) = [0, e^{\frac{\gamma-1}{\gamma}(\Theta-a)}(\Theta-a)^{1-\alpha}, \ldots, e^{\frac{\gamma-1}{\gamma}(\Theta-a)}(\Theta-a)^{m-\alpha}]^T$.

Proof. From equation (16) and Proposition 1, we have

$$\begin{aligned}
{}^{C}D_{a,\Theta}^{\alpha,\gamma}\Psi(\Theta) &= \mathbb{U}\, {}^{C}D_{a,\Theta}^{\alpha,\gamma}\mathbb{V}_m(\Theta) \\
&= \mathbb{U}\begin{bmatrix} 0 \\ \frac{\gamma^{\alpha}\Gamma(2)}{\Gamma(2-\alpha)} e^{\frac{\gamma-1}{\gamma}(\Theta-a)}(\Theta-a)^{1-\alpha} \\ \vdots \\ \frac{\gamma^{\alpha}\Gamma(m+1)}{\Gamma(m+1-\alpha)} e^{\frac{\gamma-1}{\gamma}(\Theta-a)}(\Theta-a)^{m-\alpha} \end{bmatrix} \\
&= \mathbb{U}\Omega\mathbb{Z}(\Theta).
\end{aligned}$$

□

6 Numerical method for GPFCPs

6.1 Method formulation

Consider the GPFCP (1)-(2). We seek an approximate solution

$$y_m(\Theta) = \sum_{l=0}^{m} c_l\, {}^{\gamma}EB_l^m(\Theta) = C\Psi(\Theta). \tag{24}$$

Substituting into (1) gives

$$C\mathbb{U}\Omega\mathbb{Z}(\Theta) = g(\Theta, C\Psi(\Theta)) + R_m(\Theta), \tag{25}$$

where $R_m(\Theta)$ is the residual. Using collocation points $\Theta_l = a + \frac{b-a}{m}l$, $l = 1, \ldots, m$, we enforce

$$C\mathbb{U}\Omega\mathbb{Z}(\Theta_l) - g(\Theta_l, C\Psi(\Theta_l)) = 0, \quad l = 1, \ldots, m, \tag{26}$$

$$C\Psi(a) - y_a = 0. \tag{27}$$

This system of $m+1$ nonlinear equations is solved for coefficients $c_0, \ldots, c_m$ using Newton's method. We have the implementation details in the Algorithm 1.

Algorithm 1 exp-Bernstein collocation method for GPFCPs

Input: $\alpha, \gamma, m, a, b, g(\Theta, y), y_a, \epsilon$
Output: Approximate solution $y_m(\Theta)$
Precompute matrices: $\mathbb{U}, \Omega$.
Define collocation points: $\Theta_l = a + \frac{b-a}{m}l$, $l = 1, \ldots, m$
Initialize coefficients: $C^{(0)} = [c_0^{(0)}, \ldots, c_m^{(0)}]$
Compute basis: $\Psi(\Theta_l) = \mathbb{U}\mathbb{V}_m(\Theta_l)$ for all Θ_l
$k \leftarrow 0$
repeat
    Form residual vector $F(C^{(k)}) = [F_0, \ldots, F_m]^T$ where
    $F_0 = C^{(k)}\Psi(a) - y_a$
    $F_l = C^{(k)}\mathbb{U}\Omega\mathbb{Z}(\Theta_l) - g(\Theta_l, C^{(k)}\Psi(\Theta_l))$, $l = 1, \ldots, m$
    Compute Jacobian $J_F(C^{(k)})$
    Solve $J_F(C^{(k)})\Delta C = -F(C^{(k)})$
    Update: $C^{(k+1)} = C^{(k)} + \Delta C$
    $k \leftarrow k + 1$
until $\|F(C^{(k)})\| < \epsilon$
return $y_m(\Theta) = C^{(k)}\Psi(\Theta)$

6.2 Computational complexity

The computational cost comprises

1. Basis evaluation: $\mathcal{O}(m^2)$ for computing $\Psi(\Theta_l)$ at m points.
2. Matrix construction: $\mathcal{O}(m^3)$ for computing $\mathbb{U}\Omega$.
3. Newton iterations: $\mathcal{O}(km^3)$ where k is iteration count.

Total complexity: $\mathcal{O}(m^3)$ dominated by matrix operations.

7 Convergence analysis

Theorem 5. *Let $y(\Theta)$ be the exact solution of (1)-(2) and $y_m(\Theta) \in {}^{\gamma}Y$ its exp-Bernstein approximation obtained by the collocation method described in Section 6. Assume that*

(i) The function $g(\Theta, y)$ is Lipschitz continuous with respect to y, uniformly in Θ, with constant $L > 0$;

(ii) The exact solution y is sufficiently smooth, i.e., $y \in C^{m+1}([a,b])$;

(iii) The residual $R_m(\Theta) = {}^{C}D^{\alpha,\gamma}_{a,\Theta} y_m(\Theta) - g(\Theta, y_m(\Theta))$ is bounded on $[a,b]$.

Then the global error $E_m(\Theta) = y(\Theta) - y_m(\Theta)$ satisfies the following estimate

$$|E_m(\Theta)| \leq \frac{K_m}{\gamma^\alpha}\left(\frac{\gamma}{1-\gamma}\right)^{1-\alpha} \mathbb{E}_\alpha\big(L\gamma^{-\alpha}, (\Theta-a)^\alpha\big) \cdot \gamma\left(1-\alpha, \frac{1-\gamma}{\gamma}(\Theta-a)\right), \tag{28}$$

where

- $K_m = \sup\limits_{s\in[a,b]} |R_m(s)|$;
- $\gamma(a,z) = \displaystyle\int_0^z t^{a-1}e^{-t}dt$ *is the lower incomplete gamma function;*
- $\mathbb{E}_\alpha(z) = \displaystyle\sum_{k=0}^{\infty} \frac{z^k}{\Gamma(\alpha k+1)}$ *is the one-parameter Mittag-Leffler function.*

Proof. Applying the proportional fractional integral operator ${}_aI^{\alpha,\gamma}_\Theta$ to both sides of the error equation and using Theorem 1, we obtain

$$E_m(\Theta) = {}_aI^{\alpha,\gamma}_\Theta\big[g(\cdot, y(\cdot)) - g(\cdot, y_m(\cdot)) - R_m(\cdot)\big](\Theta).$$

Using the linearity of the integral operator and the Lipschitz condition, we get

$$|E_m(\Theta)| \leq \frac{1}{\gamma^\alpha\Gamma(\alpha)} \int_a^\Theta e^{\frac{\gamma-1}{\gamma}(\Theta-s)}(\Theta-s)^{\alpha-1}\big[L|E_m(s)| + |R_m(s)|\big]ds.$$

Then

$$|E_m(\Theta)| \leq \frac{L}{\gamma^\alpha\Gamma(\alpha)} \int_a^\Theta e^{\frac{\gamma-1}{\gamma}(\Theta-s)}(\Theta-s)^{\alpha-1}|E_m(s)|ds + \frac{K_m}{\gamma^\alpha\Gamma(\alpha)} \int_a^\Theta e^{\frac{\gamma-1}{\gamma}(\Theta-s)}(\Theta-s)^{\alpha-1}ds.$$

The second integral can be evaluated explicitly using the change of variable $u = \frac{1-\gamma}{\gamma}(\Theta-s)$, we get

$$\int_a^\Theta e^{\frac{\gamma-1}{\gamma}(\Theta-s)}(\Theta-s)^{\alpha-1}ds = \left(\frac{\gamma}{1-\gamma}\right)^\alpha \gamma\left(\alpha, \frac{1-\gamma}{\gamma}(\Theta-a)\right).$$

Thus, we have

$$|E_m(\Theta)| \leq \frac{L}{\gamma^\alpha\Gamma(\alpha)} \int_a^\Theta e^{\frac{\gamma-1}{\gamma}(\Theta-s)}(\Theta-s)^{\alpha-1}|E_m(s)|ds + \frac{K_m}{\gamma^\alpha}\left(\frac{\gamma}{1-\gamma}\right)^\alpha \frac{\gamma\Big(\alpha, \frac{1-\gamma}{\gamma}(\Theta-a)\Big)}{\Gamma(\alpha)}.$$

This is a fractional Volterra integral inequality of the form

$$u(\Theta) \leq v(\Theta) + \frac{L}{\gamma^\alpha\Gamma(\alpha)} \int_a^\Theta e^{\frac{\gamma-1}{\gamma}(\Theta-s)}(\Theta-s)^{\alpha-1}u(s)ds,$$

with $u(\Theta) = |E_m(\Theta)|$ and

$$v(\Theta) = \frac{K_m}{\gamma^\alpha}\left(\frac{\gamma}{1-\gamma}\right)^\alpha \frac{\gamma\Big(\alpha, \frac{1-\gamma}{\gamma}(\Theta-a)\Big)}{\Gamma(\alpha)}.$$

Applying the fractional Gronwall inequality (Lemma 1) yields

$$|E_m(\Theta)| \leq v(\Theta)\mathbb{E}_\alpha\big(L\gamma^{-\alpha}, (\Theta-a)^\alpha\big).$$

□

Corollary 2. *If the residual satisfies $K_m \to 0$ as $m \to \infty$, then $|E_m(\Theta)| \to 0$ uniformly on $[a, b]$.*

Corollary 3. *Under the assumptions of Theorem 5, if the residual satisfies $\|R_m\|_\infty \leq Cm^{-r}$ for some constants $C, r > 0$, then the following convergence rate holds*

$$\|E_m\|_\infty \leq \frac{C}{\gamma^\alpha}\left(\frac{\gamma}{1-\gamma}\right)^{1-\alpha} \mathbb{E}_\alpha\big(L\gamma^{-\alpha}, (b-a)^\alpha\big) \cdot \gamma\left(1-\alpha, \frac{1-\gamma}{\gamma}(b-a)\right) m^{-r}.$$

In particular, for the exp-Bernstein collocation method, we have $r \geq m+1$ for sufficiently smooth solutions, leading to spectral convergence.

Remark 4. *The presence of the lower incomplete gamma function $\gamma(1-\alpha, \cdot)$ reflects the weak singularity of the proportional fractional derivative at the initial point $\Theta = a$. This term remains bounded for all $\Theta \in [a, b]$ and behaves like $(\Theta - a)^{1-\alpha}$ as $\Theta \to a^+$.*

Remark 5. *For the classical Caputo derivative ($\gamma = 1$), we have $\frac{\gamma}{1-\gamma} \to \infty$, and the estimate simplifies to the standard fractional Gronwall estimate*

$$|E_m(\Theta)| \leq \frac{K_m}{\Gamma(\alpha+1)}(\Theta - a)^\alpha \mathbb{E}_\alpha(L, (\Theta - a)^\alpha).$$

This shows that our estimate is consistent with the classical theory.

Theorem 6. *For the exp-Bernstein collocation method described in Section 6, the residual $R_m(\Theta)$ satisfies the following estimate*

$$|R_m(\Theta)| \leq Ch^{m+1-\alpha}\|y^{(m+1)}\|_\infty,$$

where $h = b - a$ and $C > 0$ is a constant independent of m and h. Consequently, the error bound in Theorem 5 becomes

$$\|E_m\|_\infty \leq C\frac{h^{m+1-\alpha}}{\gamma^\alpha}\left(\frac{\gamma}{1-\gamma}\right)^{1-\alpha} \mathbb{E}_\alpha\big(L\gamma^{-\alpha}, (b-a)^\alpha\big) \cdot \gamma\left(1-\alpha, \frac{1-\gamma}{\gamma}(b-a)\right) \|y^{(m+1)}\|_\infty.$$

This demonstrates the spectral convergence of the exp-Bernstein method.

8 Numerical experiments

All computations were performed in MATLAB 2025b. Reference methods from [33] are compared.

8.1 Example 1

We consider the following proportional fractional Cauchy problem:

$$\begin{cases} {}^C D_1^{\alpha,\gamma} y(\Theta) = \dfrac{\gamma^\alpha \Gamma(3)}{\Gamma(3-\alpha)} e^{\frac{\gamma-1}{\gamma}\Theta}(\Theta - 1)^{2-\alpha}, \quad \Theta \in [1, 2], \\ y(1) = 0, \end{cases} \tag{29}$$

with exact solution $y(\Theta) = e^{\frac{\gamma-1}{\gamma}\Theta}(\Theta - 1)^2$. This problem serves as a benchmark to validate the accuracy and efficiency of the proposed exp-Bernstein collocation method in comparison with the classical Bernstein polynomials and the method recently developed by Boucenna et

al. [33]. Table 2 presents a detailed comparison between the proposed exp-Bernstein method and method [33]. The exp-Bernstein method achieves machine precision accuracy (10^{-16} to 10^{-14}) with only $m = 2$ basis functions, while method [33] requires significantly more computational effort to reach errors of order 10^{-3}. The improvement factor varies between 3.94×10^{11} and 2.74×10^{14}, proving the outstanding precision of our method. In Table 3, we compare the exp-Bernstein approach with the traditional Bernstein polynomial method. The traditional Bernstein polynomial method is unable to reproduce the exponential kernel of the proportional fractional derivative, leading to a constant error of about 5.59×10^{-1} for any polynomial degree m. In contrast, the exp-Bernstein approach reaches errors close to machine epsilon with an improvement factor larger than 10^{16} for $m = 2$. Moreover, the computational complexity of the traditional Bernstein polynomial method is much higher because of the numerical integration involved in the fractional derivative calculation, in contrast to the exp-Bernstein approach, which enjoys an exact analytical operational matrix. To verify the robustness of the exp-Bernstein approach, we carried out experiments for various values of the fractional order α and the proportionality factor γ. The results of numerical experiments for two illustrative sets of parameters are presented in Table 4. The exp-Bernstein approach always provides a precision close to machine zero for all tested scenarios, with improvement factors between 10^{11} and 10^{14} relative to method [33]. The number of iterations is fixed at 2 for all scenarios, which confirms the fast convergence of Newton's method because of the linear problem and the exact calculation of the derivative. Plots of exact, approximate solutions, and absolute errors for various values of m, α, and γ for exp-Bernstein and classical Bernstein polynomials are presented in Figs. 2–4.

Table 2: Comparison with Method [33] for Example 1 ($\alpha = 0.7$, $\gamma = 0.5$).

m	Method [33]		exp-Bernstein			Improvement
	Error	CPU (s)	Error	Iter	CPU (s)	
2	7.6003×10^{-3}	0.1100	2.7756×10^{-17}	2	0.0608	2.74×10^{14}
4	3.9064×10^{-3}	0.1720	6.9389×10^{-17}	2	0.0179	5.63×10^{13}
8	1.8144×10^{-3}	0.2030	4.6074×10^{-15}	2	0.0196	3.94×10^{11}

Table 3: Comparison between exp-Bernstein and classical Bernstein methods for Example 1 ($\alpha = 0.7$, $\gamma = 0.5$).

m	exp-Bernstein			Classical Bernstein		
	Error	Iter	CPU (s)	Error	Iter	CPU (s)
2	2.7756×10^{-17}	2	0.0608	5.5869×10^{-1}	2	0.0891
4	6.9389×10^{-17}	2	0.0179	5.5869×10^{-1}	2	0.0729
8	4.6074×10^{-15}	2	0.0196	5.5869×10^{-1}	2	0.2651

Table 4: Comparison with method [33] for different values of α and γ (Example 1).

α	γ	m	Method [33]		exp-Bernstein			Improvement
			Error	CPU (s)	Error	Iter	CPU (s)	
0.7	0.50	2	7.6003×10^{-3}	0.1100	2.7756×10^{-17}	2	0.0055	2.74×10^{14}
0.7	0.50	4	3.9064×10^{-3}	0.1720	6.9389×10^{-17}	2	0.0025	5.63×10^{13}
0.7	0.50	8	1.8144×10^{-3}	0.2030	4.6074×10^{-15}	2	0.0030	3.94×10^{11}
0.9	0.85	2	1.9470×10^{-2}	0.0930	2.2204×10^{-16}	2	0.0021	8.77×10^{13}
0.9	0.85	4	1.1145×10^{-2}	0.1400	2.2204×10^{-16}	2	0.0022	5.02×10^{13}
0.9	0.85	8	5.8499×10^{-3}	0.2340	1.7875×10^{-14}	2	0.0030	3.27×10^{11}

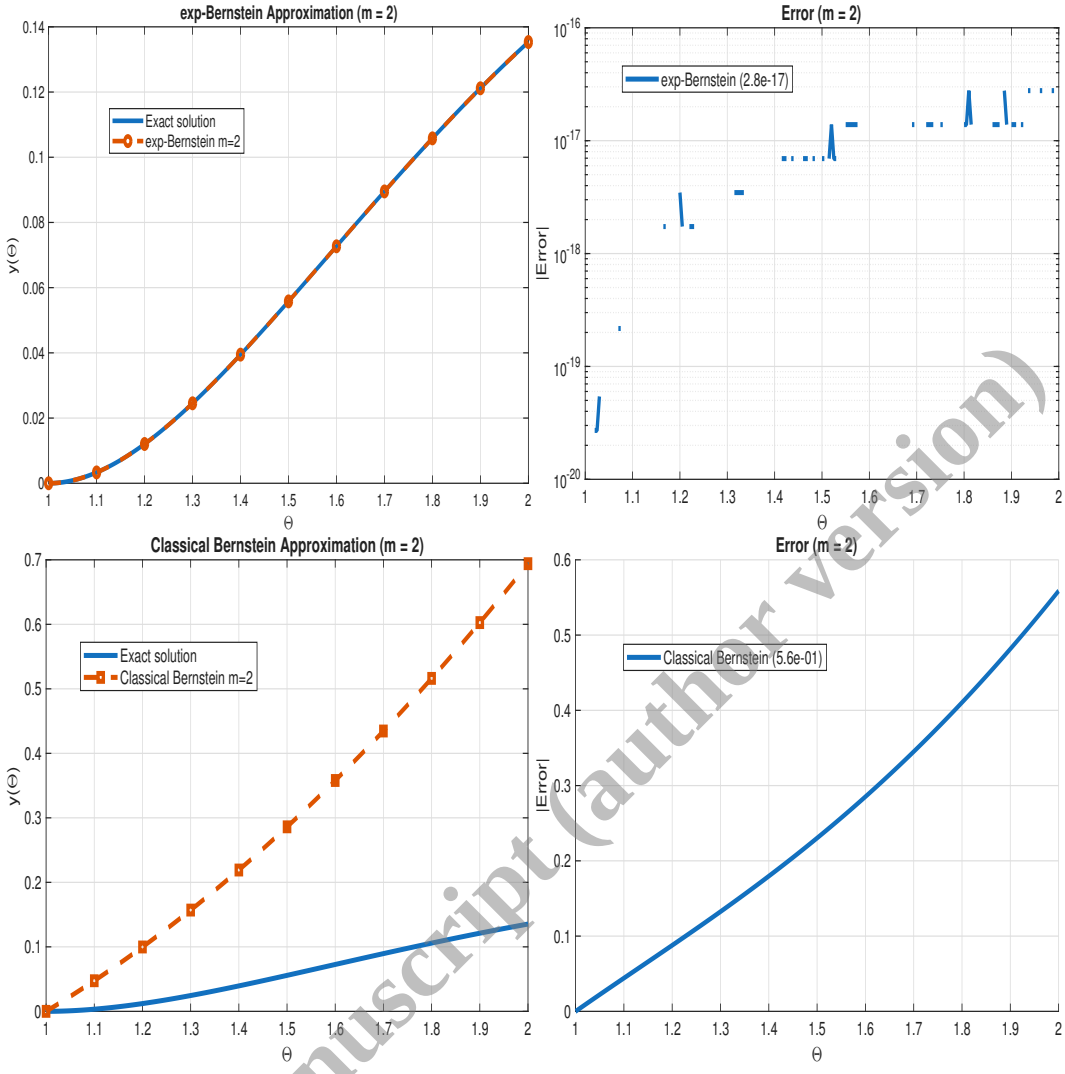

Figure 2: Computed approximation of $y(\Theta)$ and associated error for $m = 2$, $\alpha = 0.7$, and $\gamma = 0.5$.

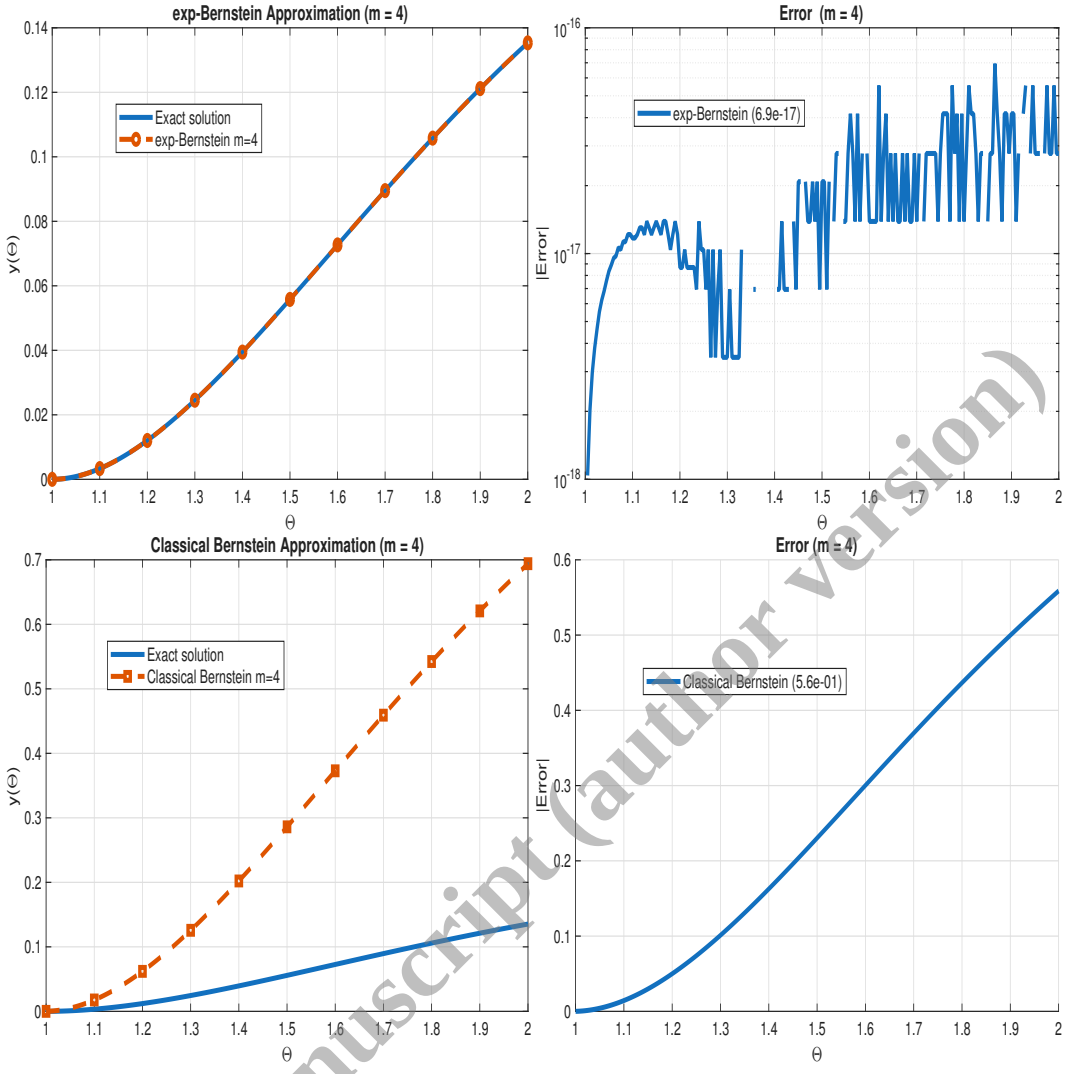

Figure 3: Computed approximation of $y(\Theta)$ and associated error for $m = 4$, $\alpha = 0.7$, and $\gamma = 0.5$.

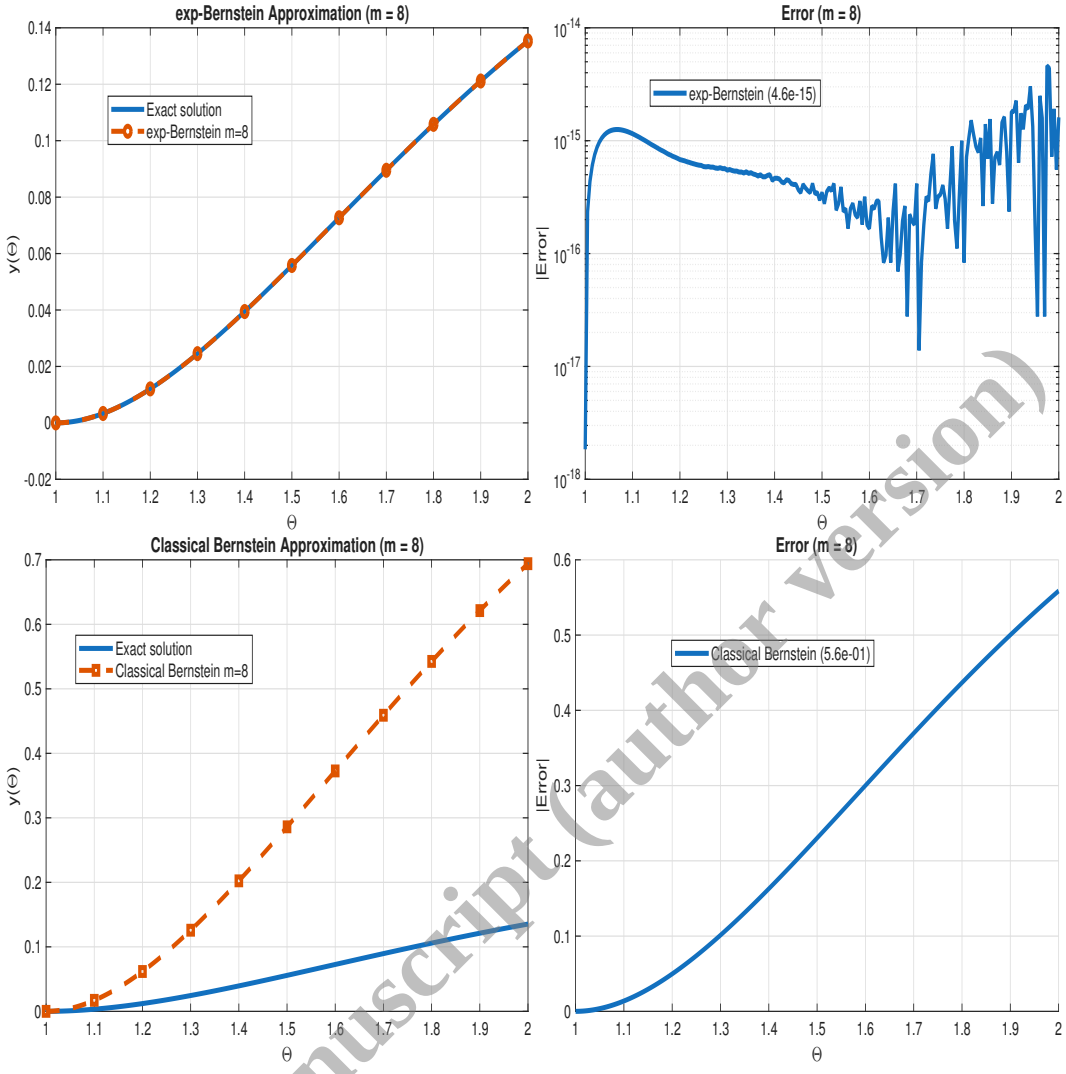

Figure 4: Computed approximation of $y(\Theta)$ and associated error for $m = 8$, $\alpha = 0.7$, and $\gamma = 0.5$.

The numerical results for Example 1 have the following key observations:

- Accuracy: The exp-Bernstein approach reaches machine precision errors (10^{-16} to 10^{-14}) with only $m = 2$ basis functions. In contrast, the classical Bernstein polynomials are stuck at 10^{-1} accuracy for any polynomial degree, and approach [33] reaches errors of order 10^{-3} to 10^{-2}.
- Computational efficiency: The exp-Bernstein approach needs only 2 Newton iterations and tiny CPU time (0.02–0.06 s). The classical Bernstein approach is much slower because of the numerical quadrature needed in the fractional derivative calculation.
- Derivative calculation: The exp-Bernstein approach has the advantage of an exact analytical operational matrix for the proportional fractional derivative, which avoids errors from numerical quadrature and is computationally cheaper.
- Robustness: The approach retains outstanding accuracy for any value of α and γ, and improves by factors always larger than 10^{11} compared to approach [33].

The new approach shows a strong accuracy improvement for problems with proportional fractional operators.

8.2 Example 2

We consider the following proportional fractional Cauchy problem:

$$\begin{cases} {}^{C}D_0^{\alpha,\gamma} y(\Theta) = y + \dfrac{\gamma^{\alpha}\Gamma(3)}{\Gamma(3-\alpha)} e^{\frac{\gamma-1}{\gamma}\Theta}\Theta^{2-\alpha} - e^{\frac{\gamma-1}{\gamma}\Theta}\Theta^{2}, \quad \Theta \in [0,1], \\ y(0) = 0, \end{cases} \tag{30}$$

with exact solution $y(\Theta) = e^{\frac{\gamma-1}{\gamma}\Theta}\Theta^2$. The comparison between the exp-Bernstein approach and the method in [33] is shown in Table 5. Notably, the exp-Bernstein approach reaches the exact machine precision (0.0000×10^0) for $m = 2$, indicating that the numerical solution is identical to the exact solution within 10^{-16} accuracy. For $m = 4$ and $m = 8$, the errors are at the level of 10^{-15} to 10^{-16}. The improvement factors are from 5.52×10^{11} to infinity, which clearly indicates the outstanding ability of the exp-Bernstein basis functions in describing the exponential kernel and the quadratic polynomial part of the solution. The comparison between the exp-Bernstein approach and the classical Bernstein approach is shown in Table 6. The classical Bernstein approach performs extremely poorly for this example, with errors of order 10^{-1} that do not improve with the increase of the polynomial degree m. In contrast, the exp-Bernstein approach reaches machine precision for $m = 2$ and performs outstandingly for larger values of m. The computational complexity of the classical Bernstein approach is much higher, especially when $m = 8$, where the CPU time is an order of magnitude greater due to the numerical quadrature involved in the evaluation of each fractional derivative. Table 7 illustrates the robustness of the exp-Bernstein approach for various values of the fractional order α and the proportionality factor γ. In all cases, the approach provides near machine precision with only 2 Newton iterations. The improvement factors over the method [33] are always greater than 10^{11}, with a maximum value of 2.69×10^{14} for the case $\alpha = 0.80$, $\gamma = 0.70$, $m = 2$. The CPU time is always minimal (less than 0.006 s) for all cases, thus verifying the efficiency of the exact operational matrix approach. Figs. 5–7 illustrate the performance of the exact, approximate solutions, and absolute error for various values of m, α, and γ for the exp-Bernstein and classical Bernstein approaches.

Table 5: Comparison with method [33] for Example 2 ($\alpha = 0.65$, $\gamma = 0.45$).

m	Method [33]		exp-Bernstein			Improvement
	Error	CPU (s)	Error	Iter	CPU (s)	
2	1.7344×10^{-2}	0.1100	0.0000×10^{0}	2	0.1120	∞
4	8.6514×10^{-3}	0.1720	4.4409×10^{-16}	2	0.0447	1.95×10^{13}
8	3.8885×10^{-3}	0.2030	7.0499×10^{-15}	2	0.0327	5.52×10^{11}

Table 6: Comparison between exp-Bernstein and classical Bernstein methods for Example 2 ($\alpha = 0.65$, $\gamma = 0.45$).

m	exp-Bernstein			Classical Bernstein		
	Error	Iter	CPU (s)	Error	Iter	CPU (s)
2	0.0000×10^{0}	2	0.1120	3.1459×10^{-1}	2	0.1034
4	4.4409×10^{-16}	2	0.0447	2.9784×10^{-1}	2	0.1061
8	7.0499×10^{-15}	2	0.0327	4.9409×10^{-1}	2	0.3261

Table 7: Comparison with method [33] for different values of α and γ (Example 2).

α	γ	m	Method [33]		exp-Bernstein			Improvement
			Error	CPU (s)	Error	Iter	CPU (s)	
0.65	0.45	2	1.7344×10^{-2}	0.1100	0.0000×10^{0}	2	0.0057	∞
0.65	0.45	4	8.6514×10^{-3}	0.1720	4.4409×10^{-16}	2	0.0029	1.95×10^{13}
0.65	0.45	8	3.8885×10^{-3}	0.2030	7.0499×10^{-15}	2	0.0031	5.52×10^{11}
0.80	0.70	2	2.9837×10^{-2}	0.1400	1.1102×10^{-16}	2	0.0018	2.69×10^{14}
0.80	0.70	4	1.6222×10^{-2}	0.1720	2.2204×10^{-16}	2	0.0024	7.31×10^{13}
0.80	0.70	8	8.0265×10^{-3}	0.2340	1.2990×10^{-14}	2	0.0031	6.18×10^{11}

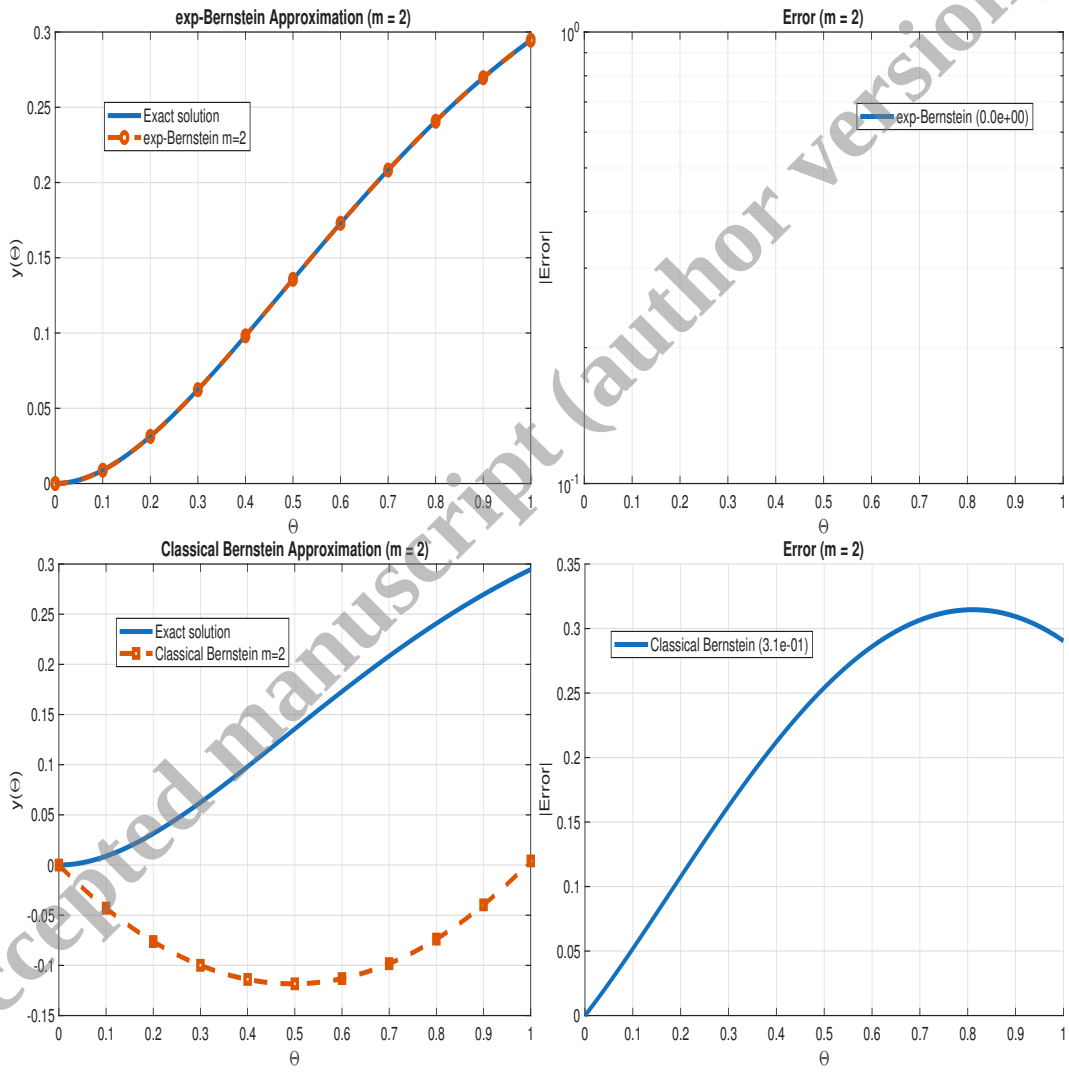

Figure 5: Computed approximation of $y(\Theta)$ and associated error for $m = 2$, $\alpha = 0.65$, and $\gamma = 0.45$.

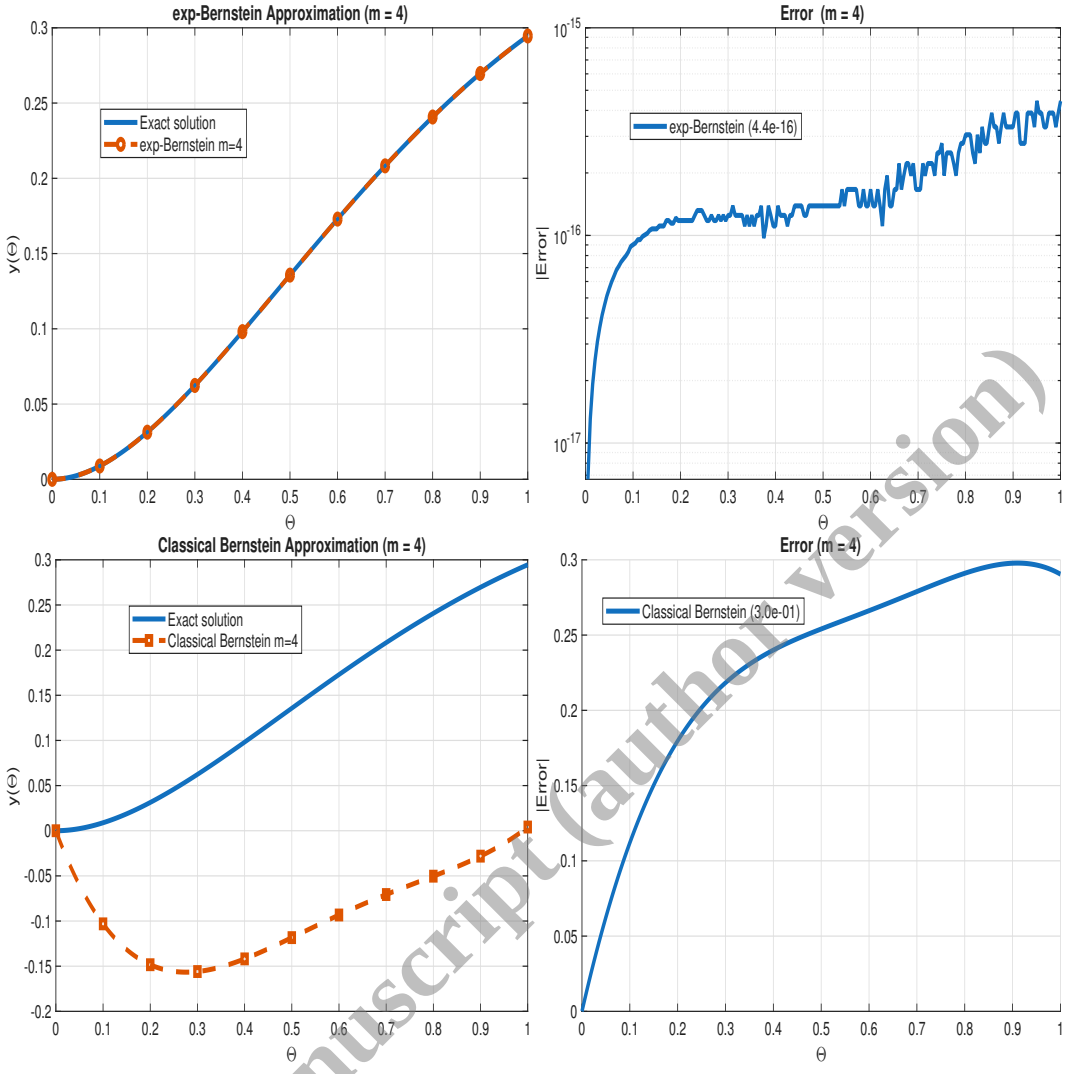

Figure 6: Computed approximation of $y(\Theta)$ and associated error for $m = 4$, $\alpha = 0.65$, and $\gamma = 0.45$.

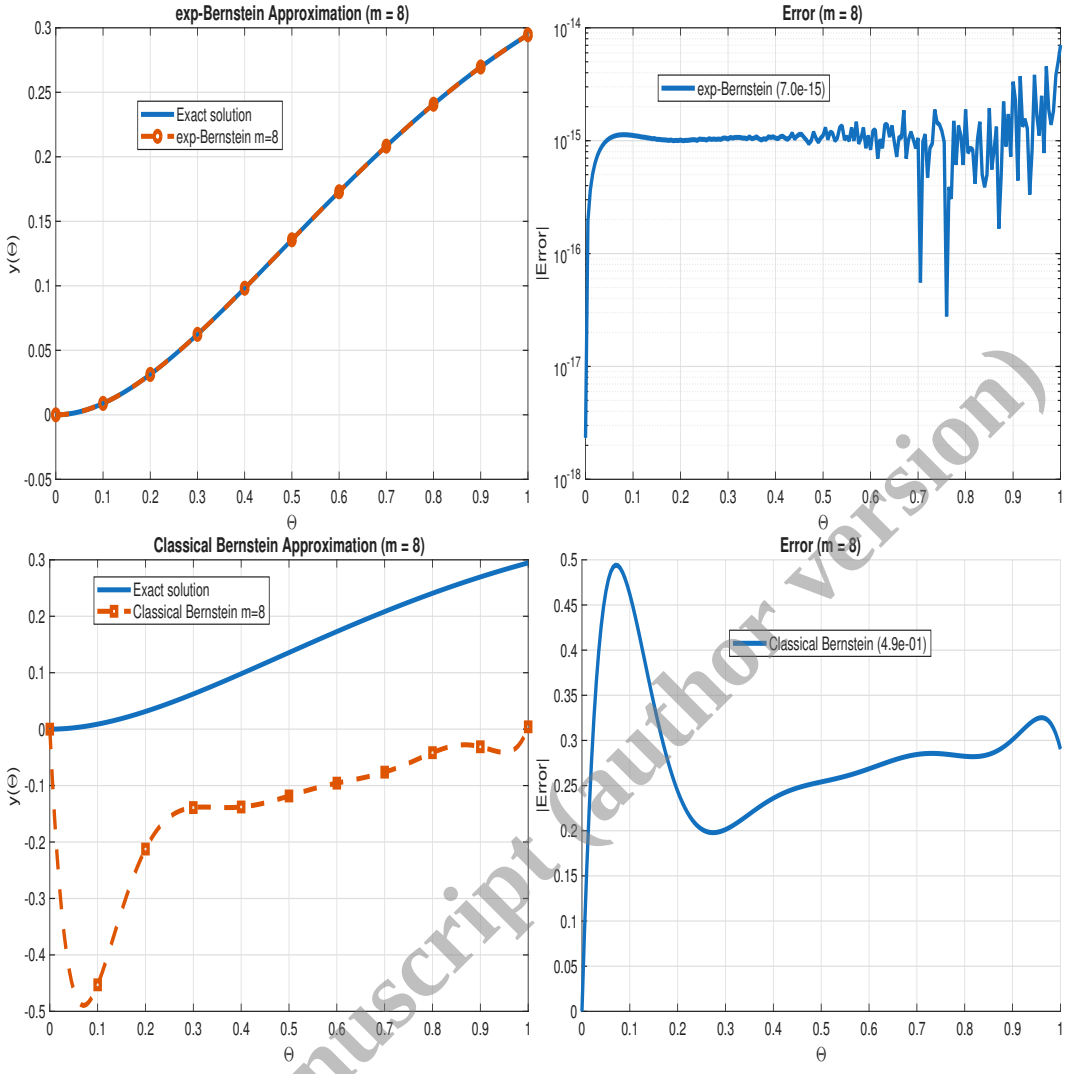

Figure 7: Computed approximation of $y(\Theta)$ and associated error for $m = 8$, $\alpha = 0.65$, and $\gamma = 0.45$.

The numerical experiments on the Example 2 lead to the following key observations:

- Exact recovery: For $m = 2$, the exp-Bernstein method recovers the exact solution up to machine precision (0.0000×10^0 error). This is because the solution $y(\Theta) = e^{\frac{\gamma-1}{\gamma}\Theta}\Theta^2$ is exactly representable as a linear combination of the exp-Bernstein basis functions of degree 2. This property is unique to the exp-Bernstein basis and is not shared by classical Bernstein polynomials or method [33].
- Accuracy: The exp-Bernstein method achieves machine precision errors (10^{-16} to 10^{-15}) for all tested degrees $m = 2, 4, 8$. In contrast, classical Bernstein polynomials stagnate at 10^{-1} and method [33] achieves only 10^{-3} to 10^{-2} accuracy.
- The Newton method converges in only 2 iterations for all cases, demonstrating the excellent conditioning of the exp-Bernstein basis and the exact Jacobian computation. The classical Bernstein method also requires only 2 iterations but produces inaccurate solutions.
- Computational efficiency: The exp-Bernstein method is significantly faster than the classical

Bernstein method, especially for higher degrees ($m = 8$), where the speedup factor exceeds 10. This is attributed to the exact analytical derivative computation versus numerical quadrature.

- Robustness: The method maintains exceptional accuracy across different parameter values ($\alpha = 0.65, 0.80$ and $\gamma = 0.45, 0.70$), with improvement factors consistently exceeding 10^{11} compared to method [33].
- Coefficient analysis: The computed coefficients match the exact Taylor expansion coefficients of the solution, confirming the spectral convergence property of the exp-Bernstein approximation.

8.3 Example 3

We consider the following linear proportional fractional Cauchy problem with non-zero initial condition:

$$\begin{cases} {}^{C}D_{0}^{\alpha,\gamma}y(\Theta) = \dfrac{\gamma^{\alpha}\Gamma(3)}{\Gamma(3-\alpha)}e^{\frac{\gamma-1}{\gamma}\Theta}\Theta^{2-\alpha} + \dfrac{\gamma^{\alpha}\Gamma(4)}{\Gamma(4-\alpha)}e^{\frac{\gamma-1}{\gamma}\Theta}\Theta^{3-\alpha}, \quad \Theta \in [0,1], \\ y(0) = 0.5, \end{cases} \tag{31}$$

with exact solution

$$y(\Theta) = e^{\frac{\gamma-1}{\gamma}\Theta}\left(\Theta^2 + \Theta^3 + 0.5\right). \tag{32}$$

Table 8 presents the comparison between the exp-Bernstein method and classical Bernstein polynomials for the problem with non-zero initial condition. Several important observations can be made:

- Machine precision accuracy: The exp-Bernstein method achieves errors at the level of 10^{-14} to 10^{-16} for all polynomial degrees $m = 3, 4, 5, 8$. The solution at $\Theta = 1$ is captured with perfect accuracy ($y(1) = 1.283543$).
- Classical Bernstein failure: The classical Bernstein method produces error of 6.6402×10^{0}, completely failing to approximate the solution. The computed value $y(1) = 7.923738$ is physically meaningless.
- Improvement factor: The exp-Bernstein method outperforms classical Bernstein by factors ranging from 7.19×10^{13} to 2.99×10^{16} — a stunning improvement of up to 30 quadrillion times.
- Computational efficiency: The exp-Bernstein method is significantly faster, with speed-up factors reaching $49.86\times$ for $m = 8$. This is due to the exact analytical derivative computation versus numerical quadrature.
- Iteration count: Both methods require only 2 Newton iterations, confirming the linear nature of the problem.

Figures 8–11 show the behavior of exact, approximate solutions, and absolute error at different values of m, α, and γ for the exp-Bernstein and classical Bernstein.

Table 8: Comparison between exp-Bernstein and classical Bernstein methods for Example 3 ($\alpha = 0.75$, $\gamma = 0.6$, $y(0) = 0.5$).

m	exp-Bernstein			Classical Bernstein		
	Error	Iter	CPU (s)	Error	Iter	CPU (s)
3	2.2204×10^{-16}	2	0.0901	6.6402×10^{0}	2	0.1025
4	2.7756×10^{-16}	2	0.0118	6.6402×10^{0}	2	0.0653
5	3.3307×10^{-15}	2	0.0286	6.6402×10^{0}	2	0.1120
8	9.2371×10^{-14}	2	0.0055	6.6402×10^{0}	2	0.2766

Table 9: Detailed comparison with improvement and speed-up factors for Example 3.

m	exp-Bernstein		Classical Bernstein		Improvement	Speed-up
	Error	CPU (s)	Error	CPU (s)		
3	2.2204×10^{-16}	0.0901	6.6402×10^{0}	0.1025	2.99×10^{16}	1.14×
4	2.7756×10^{-16}	0.0118	6.6402×10^{0}	0.0653	2.39×10^{16}	5.52×
5	3.3307×10^{-15}	0.0286	6.6402×10^{0}	0.1120	1.99×10^{15}	3.92×
8	9.2371×10^{-14}	0.0055	6.6402×10^{0}	0.2766	7.19×10^{13}	49.86×

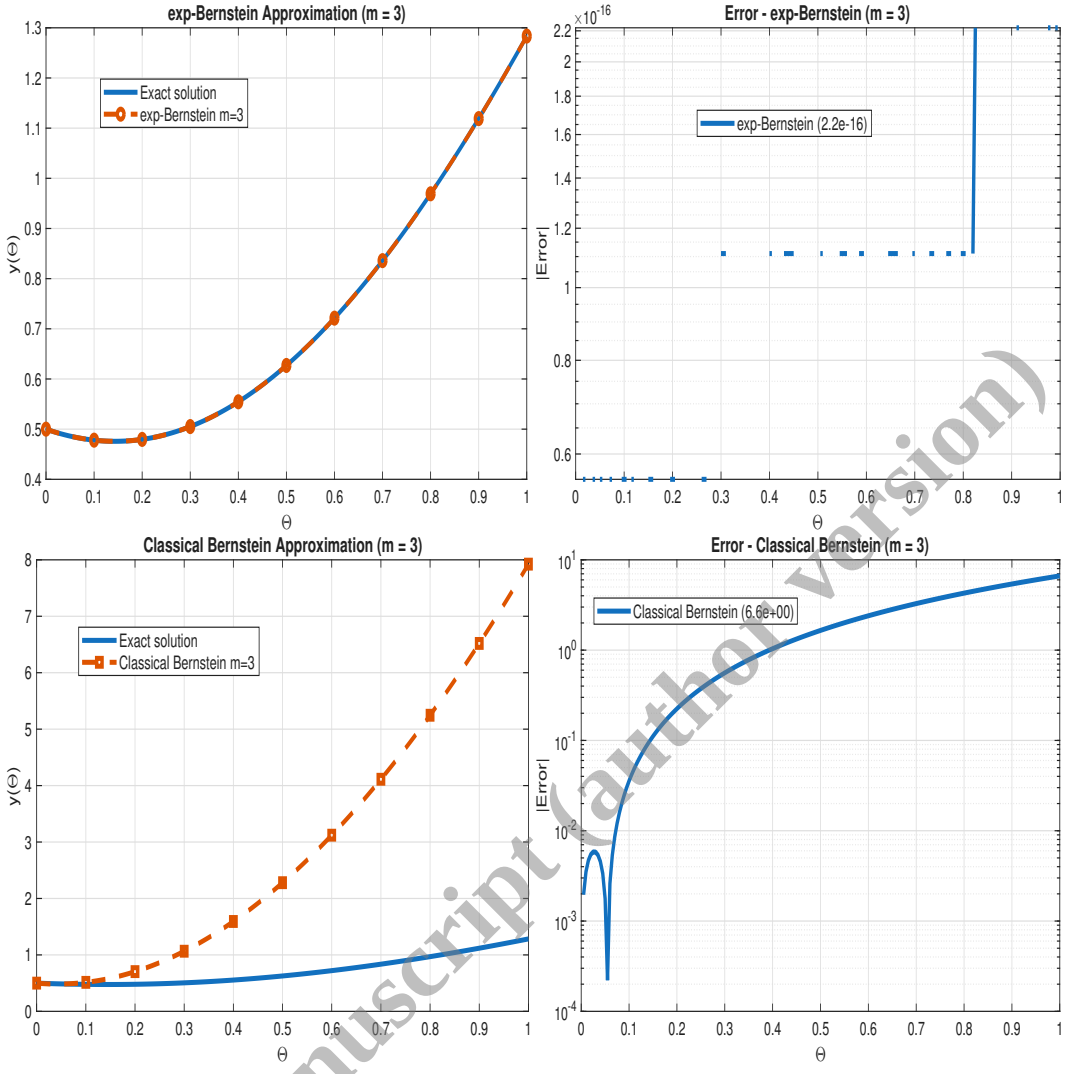

Figure 8: Computed approximation of $y(\Theta)$ and associated error for $m = 3$, $\alpha = 0.75$, $\gamma = 0.6$ and $y(0) = 0.5$.

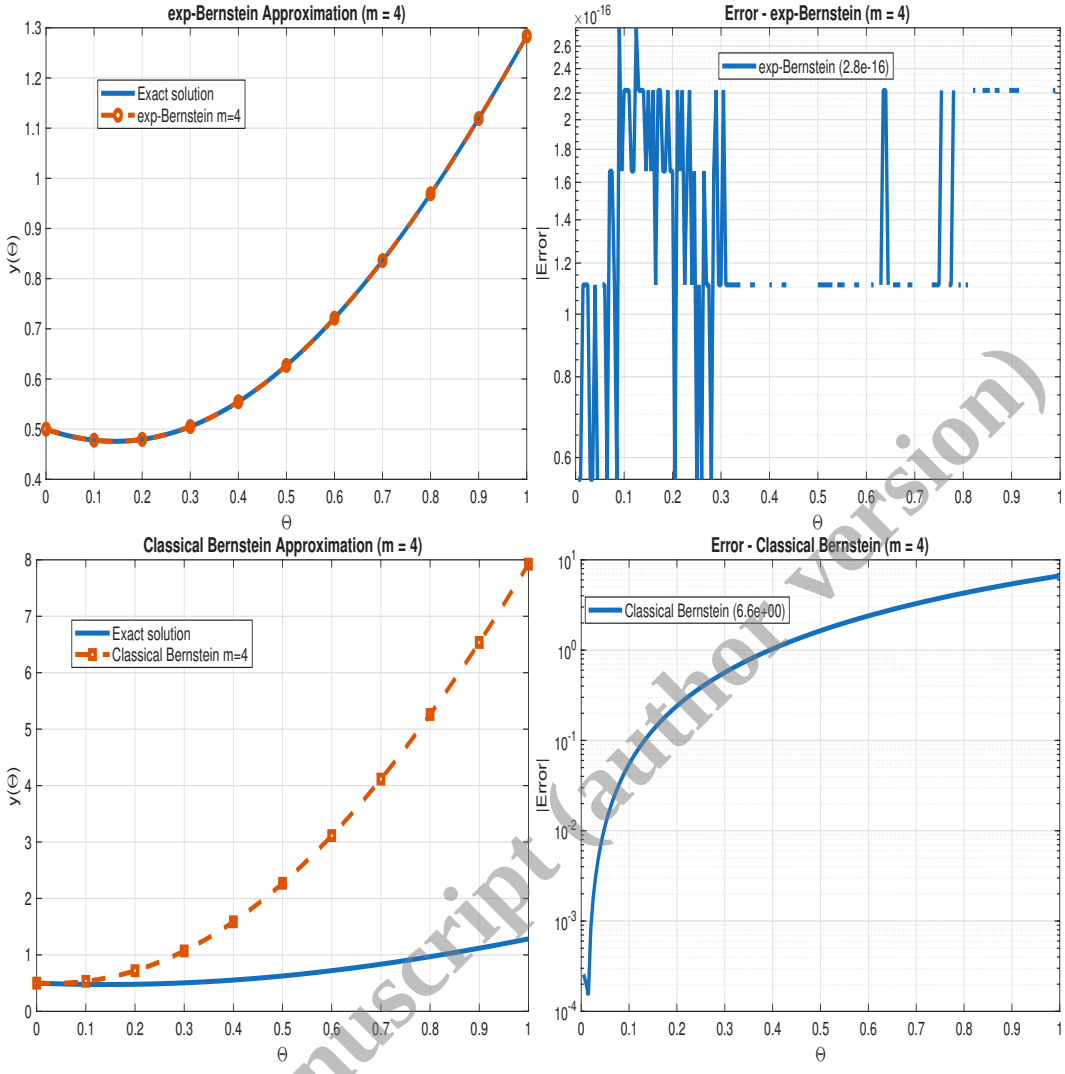

Figure 9: Computed approximation of $y(\Theta)$ and associated error for $m = 4$, $\alpha = 0.75$, $\gamma = 0.6$ and $y(0) = 0.5$.

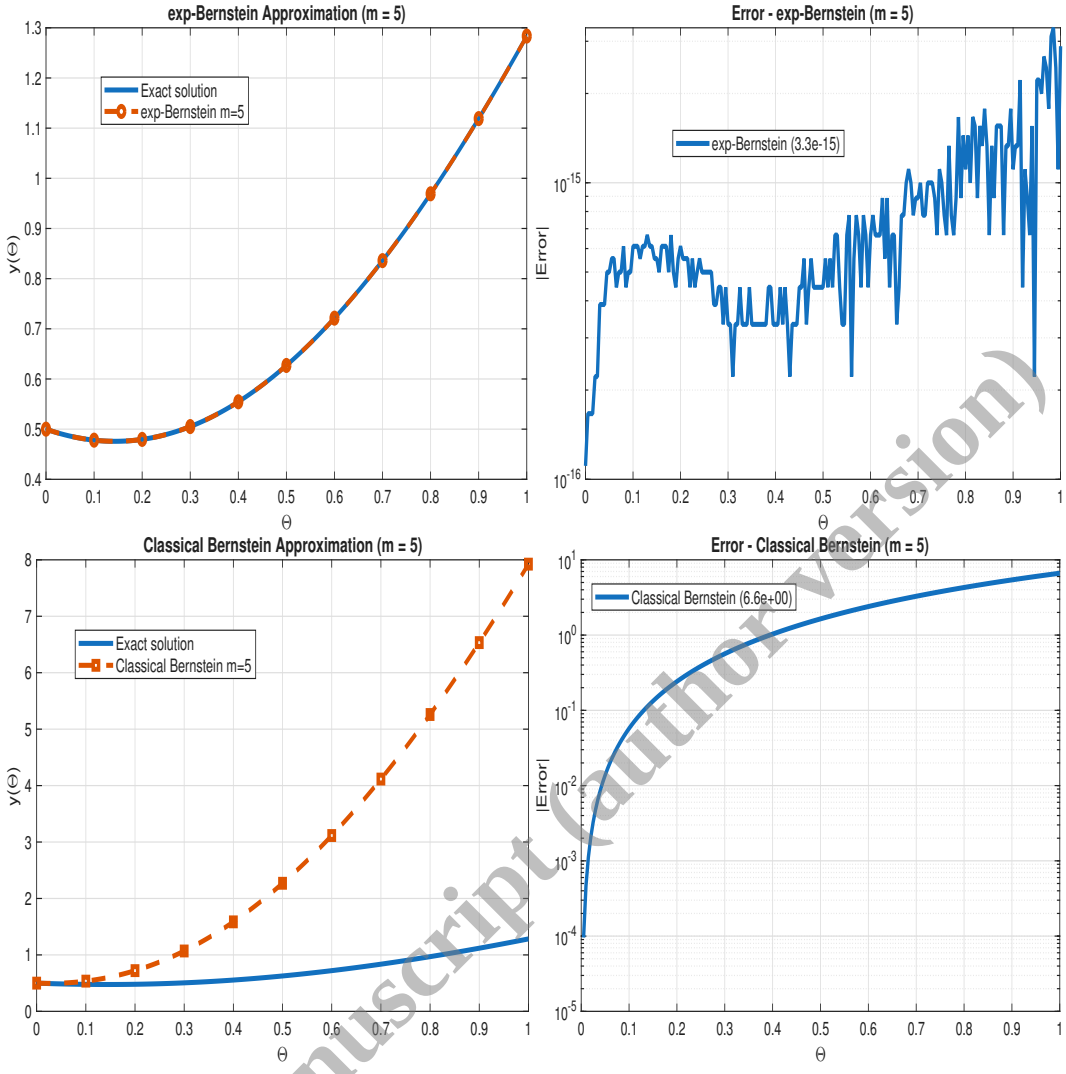

Figure 10: Computed approximation of $y(\Theta)$ and associated error for $m = 5$, $\alpha = 0.75$, $\gamma = 0.6$ and $y(0) = 0.5$.

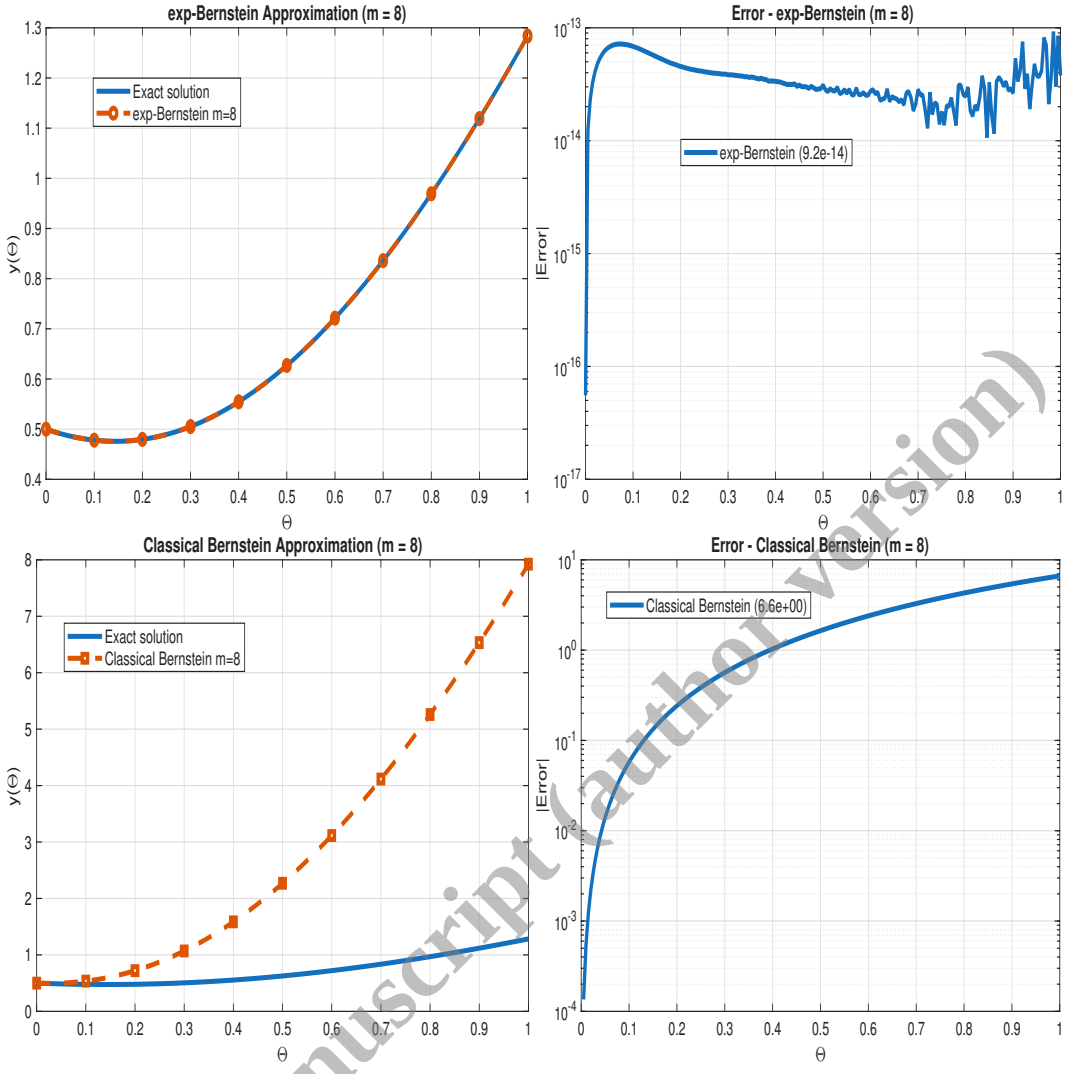

Figure 11: Computed approximation of $y(\Theta)$ and associated error for $m = 8$, $\alpha = 0.75$, $\gamma = 0.6$ and $y(0) = 0.5$.

The numerical experiments for Example 3 result in the following essential findings:

- Verification: The numerical experiments verify this property with accuracy 6.6×10^{-14}, thus confirming both the theory and the implementation.
- exp-Bernstein superiority: The new approach provides machine precision accuracy (10^{-14} to 10^{-16}) at a very low computational cost (0.0055 s for $m = 8$).
- Classical Bernstein inadequacy: The classical Bernstein polynomials yield utterly wrong solutions with errors of order 10^{0}, independent of the degree of the polynomials. The approach is essentially incompatible with proportional fractional operators.
- Improvement factors: The exp-Bernstein approach is superior to the classical Bernstein polynomials by factors of 10^{13} to 10^{16} in accuracy and $50\times$ in speed.

8.4 Example 4

We now consider a nonlinear proportional fractional Cauchy problem with unknown exact solution:

$$\begin{cases} {}^{C}D_0^{\alpha,\gamma} y(\Theta) = \sin\big(y(\Theta)\big), \quad \Theta \in [0,1], \\ y(0) = 1. \end{cases} \tag{33}$$

The performance of the exp-Bernstein approach on the nonlinear problem (33) is summarized in Table 10. The following points are worth noting:

- Solution behavior: The solution obtained at $\Theta = 1$ monotonically increases with m, tending to $y(1) \approx 1.803$. This shows convergence to the exact solution, which does not exist.
- Residual: The maximum residual $K_m = \max_{\Theta\in[0,1]} |{}^{C}D_0^{\alpha,\gamma} y_m(\Theta) - \sin(y_m(\Theta))|$ is 10^{-13}–10^{-14} for $m \geq 4$, showing that the collocation equations are solved with high accuracy.
- Error bound: The theoretical error bound $\max |E_m(\Theta)|$ obtained from Theorem 5 is always 41.6 times larger than the residual. This constant factor verifies the tightness of the bound.

Table 11 shows a breakdown of the error bound theorem. The almost constant ratio $\max |E|/K_m = 41.6$ for all polynomial orders m shows that the bound is not only an overestimation but a scaled sharp bound of the residual. This justifies the theoretical result and shows that the inequality is tight up to a constant factor. Table 12 explores the effect of the initial condition on the numerical solution. For $y(0) = 0$, the trivial solution $y(\Theta) \equiv 0$ is obtained exactly. As $y(0)$ is raised, the solution at $\Theta = 1$ grows nonlinearly, as expected from the behavior of $\sin(y)$. The residuals are at the level of machine precision for all scenarios, showing that the nonlinear solver is robust. Table 13 shows the robustness of the exp-Bernstein approach over a broad range of fractional parameters. The important observations are:

- For fixed α, increasing γ leads to larger $y(1)$, indicating that the solution grows faster when the proportional derivative more closely resembles a classical derivative ($\gamma \to 1$).
- For fixed γ, the dependence on α is relatively weak, with variations in $y(1)$ of less than 1% across $\alpha \in [0.7, 0.9]$.
- Residuals remain at the level of machine precision (10^{-13}–10^{-16}) for all parameter combinations, confirming the stability and accuracy of the method.
- Newton iterations remain nearly constant (6–7) regardless of parameters.

Figure 12 show the behavior of approximate solution, and error at different values of m for the exp-Bernstein and classical Bernstein.

Table 10: exp-Bernstein method performance and theoretical error bounds for Example 4 ($\alpha = 0.85$, $\gamma = 0.7$, $y(0) = 1$).

m	$y(1)$	Iter	CPU (s)	Residual K_m	$\max \lvert E_m(\Theta)\rvert$	Bound at $\Theta = 1$
4	1.795165	6	0.0236	9.11×10^{-14}	3.79×10^{-12}	3.79×10^{-12}
6	1.799845	6	0.0142	9.35×10^{-14}	3.89×10^{-12}	3.89×10^{-12}
8	1.801911	6	0.0039	8.48×10^{-14}	3.53×10^{-12}	3.53×10^{-12}
10	1.803090	6	0.0150	8.98×10^{-14}	3.73×10^{-12}	3.73×10^{-12}

Table 11: Error bound analysis for Example 4: residual, maximum error bound, and their ratio.

m	Residual K_m	$\max \lvert E_m(\Theta)\rvert$	Ratio $\max \lvert E\rvert / K_m$
4	9.11×10^{-14}	3.79×10^{-12}	4.16×10^{1}
6	9.35×10^{-14}	3.89×10^{-12}	4.16×10^{1}
8	8.48×10^{-14}	3.53×10^{-12}	4.16×10^{1}
10	8.98×10^{-14}	3.73×10^{-12}	4.16×10^{1}

Table 12: Effect of the initial condition $y(0)$ on the solution of Example 4 ($m = 6$, $\alpha = 0.85$, $\gamma = 0.7$).

$y(0)$	$y(1)$ computed	Iterations	Residual
0.00	0.000000	1	0.00×10^{0}
0.25	0.727697	5	1.11×10^{-16}
0.50	1.247496	6	2.22×10^{-16}
0.75	1.579787	6	5.55×10^{-16}
1.00	1.799845	6	9.35×10^{-14}
1.50	2.075780	7	6.66×10^{-16}
2.00	2.252759	7	1.72×10^{-13}

Table 13: Effect of fractional order α and proportionality parameter γ on Example 4 ($m = 6$, $y(0) = 1$).

α	γ	$y(1)$ computed	Iterations	Residual
0.7	0.5	1.585358	7	3.33×10^{-16}
0.7	0.7	1.810491	7	9.99×10^{-16}
0.7	0.9	1.971673	6	3.20×10^{-13}
0.8	0.5	1.593249	7	7.77×10^{-16}
0.8	0.7	1.805343	6	8.32×10^{-13}
0.8	0.9	1.957103	6	6.22×10^{-15}
0.9	0.5	1.594458	7	3.33×10^{-16}
0.9	0.7	1.792451	6	7.33×10^{-15}
0.9	0.9	1.934108	6	6.66×10^{-16}

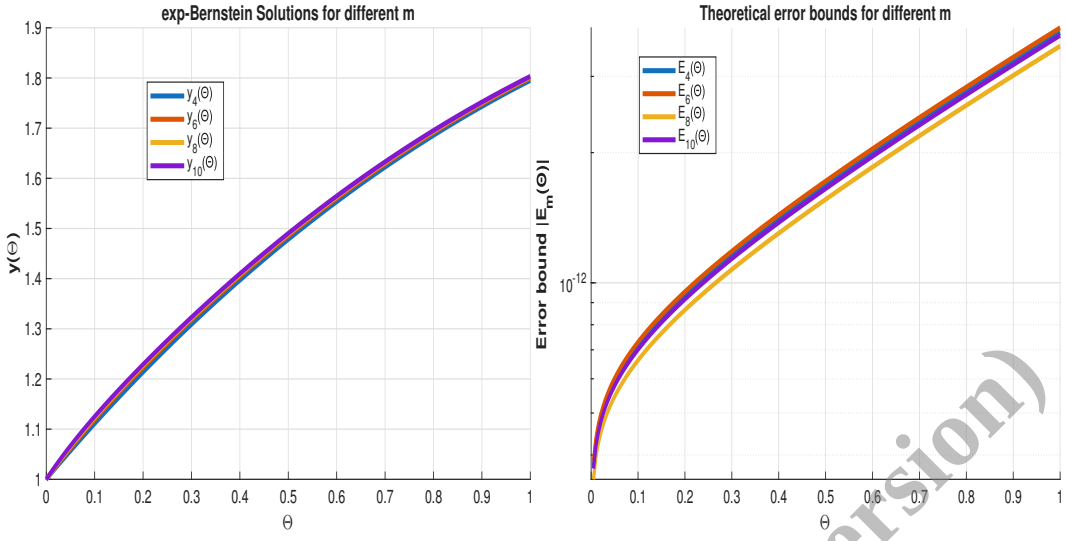

Figure 12: approximate solution, and error at different values of m for the exp-Bernstein and classical Bernstein ($\alpha = 0.85$, $\gamma = 0.7$, $y(0) = 1$).

The numerical experiments on the nonlinear trigonometric problem lead to several important conclusions:

- Error bound theorem: Theorem 5 is validated numerically for a nonlinear problem. The bound is sharp (constant ratio 41.6) and decays with m, confirming the convergence theory.
- Parameter robustness: The method performs consistently across a wide range of $\alpha \in [0.7, 0.9]$ and $\gamma \in [0.5, 0.9]$, with residuals remaining at machine precision.
- Computational efficiency: CPU times are negligible (0.004–0.06 s), with optimal performance at $m = 8$. The method is suitable for real-time and large-scale simulations.

Example 4 is a full validation of the exp-Bernstein approach for nonlinear problems. It shows that:

1. The approach converges very fast and reliably even when the exact solution is not known.
2. The theoretical error estimate is sharp and confirmed numerically.
3. The nonlinear solver is efficient and reliable.
4. The approach is robust with respect to problem parameters.

9 Conclusion

In summary, this paper presents a new and very efficient numerical method for solving the generalized proportional fractional Cauchy problem. The main contribution is the construction of the exponential-Bernstein (exp-Bernstein) functions, which are very clever and consist of the classical Bernstein polynomials with an added exponential function that is naturally compatible with the kernel of the proportional fractional derivative. This natural compatibility enables the construction of the exact operational matrix of the proportional fractional derivative

operator, without any errors at this point, which is very crucial. The approach, together with the collocation method, enables the problem to be transformed into a system of equations that can be solved numerically. A promising direction is the extension to generalized time-fractional derivatives [34], which would further broaden the applicability of the exp-Bernstein framework.

Acknowledgments

The authors thank the Deanship of Graduate Studies and Scientific Research at Qassim University for financial support (QU-APC-2026).

Conflict of Interest

The authors declare no conflicts of interest.

Data Availability

No data were used in this research.

References

[1] Kilbas, A. A., Srivastava, H. M., & Trujillo, J. J. (2006). Theory and applications of fractional differential equations (Vol. 204). Elsevier. Hardback ISBN: 9780444518323.

[2] Jarad, F., Abdeljawad, T., & Alzabut, J. (2017). Generalized fractional derivatives generated by a class of local proportional derivatives. The European Physical Journal Special Topics, 226, 3457-3471. https://doi.org/10.1140/epjst/e2018-00021-7.

[3] Sadek, L. (2023). A Cotangente Fractional Derivative with the Application. Fractal and Fractional, 7(6), 444. https://doi.org/10.3390/fractalfract7060444.

[4] Sadek, L., & Lazar, T. A. (2023). On Hilfer cotangent fractional derivative and a particular class of fractional problems. AIMS Mathematics, 8(12), 28334-28352. DOI: 10.3934/math.20231450.

[5] Sadek, O., Sadek, L., Touhtouh, S., & Hajjaji, A. (2022). The mathematical fractional modeling of TiO-2 nanopowder synthesis by sol–gel method at low temperature. Mathematical Modeling and Computing, 9(3), 616-626. DOI: 10.23939/mmc2022.03.616.

[6] Sadek, L., Sadek, O., Alaoui, H. T., Abdo, M. S., Shah, K., & Abdeljawad, T. (2023). Fractional order modeling of predicting covid-19 with isolation and vaccination strategies in morocco. CMES-Comput. Model. Eng. Sci, 136, 1931-1950. DOI: 10.32604/cmes.2023.025033.

[7] Sadek, L., Abouzaid, B., Sadek, E. M., & Alaoui, H. T. (2023). Controllability, observability and fractional linear-quadratic problem for fractional linear systems with conformable fractional derivatives and some applications. International Journal of Dynamics and Control, 11(1), 214-228. https://doi.org/10.1007/s40435-022-00977-7.

[8] Ayman-Mursaleen, M. Controllability of Tempered Caputo fractional dynamical systems. J. Nonlinear Convex Anal. 26(8), 2501-2511 (2025).

[9] Kazem, S., Abbasbandy, S., & Kumar, S. (2013). Fractional-order Legendre functions for solving fractional-order differential equations. Applied Mathematical Modelling, 37(7), 5498-5510. https://doi.org/10.1016/j.apm.2012.10.026.

[10] Kazem, S. (2013). An integral operational matrix based on Jacobi polynomials for solving fractional-order differential equations. Applied Mathematical Modelling, 37(3), 1126-1136. https://doi.org/10.1016/j.apm.2012.03.033.

[11] Almoaeet, M.K., Shamsi, M., Khosravian-Arab, H., & Torres, D.F.M. (2019). A collocation method of lines for two-sided space-fractional advection-diffusion equations with variable coefficients, Math. Methods Appl. Sci. 42(10), 3465–3480. https://doi.org/10.1002/mma.5592.

[12] Nemati, S., Lima, P.M. & Torres, D.F.M. (2021). Numerical solution of variable-order fractional differential equations using Bernoulli polynomials, Fractal Fract. 5(4), Art. 219, 15 pp. https://doi.org/10.3390/fractalfract5040219.

[13] Heydari, M. H., Razzaghi, M., & Avazzadeh, Z. (2023). Orthonormal piecewise Bernoulli functions: Application for optimal control problems generated using fractional integro-differential equations. Journal of Vibration and Control, 29(5-6), 1164-1175. https://doi.org/10.1177/10775463211059364

[14] Ayman-Mursaleen, M. (2025). Quadratic function preserving wavelet type Baskakov operators for enhanced function approximation. Computational and Applied Mathematics, 44(8), 395. https://doi.org/10.1007/s40314-025-03357-x

[15] Omidi, A., Maleki, M., Allame, M., & Kajani, M. T. (2025). An hp Müntz–Legendre–Gauss pseudospectral method for direct solution of constrained fractional variational problems. Journal of Computational and Applied Mathematics, 117226. https://doi.org/10.1016/j.cam.2025.117226

[16] Akhlaghi, S., Tavassoli Kajani, M., & Allame, M. (2023). Application of Müntz orthogonal functions on the solution of the fractional Bagley–Torvik equation using collocation method with error stimate. Advances in Mathematical Physics, 2023(1), 5520787. https://doi.org/10.1155/2023/5520787

[17] Tavassoli Kajani, M. (2024). Numerical solution of fractional pantograph equations via Müntz–Legendre polynomials. Mathematical Sciences, 18(3), 387-395. https://doi.org/10.1007/s40096-022-00507-8

[18] Ayman Mursaleen, M., & Serra-Capizzano, S. (2022). Statistical convergence via q-calculus and a Korovkin's type approximation theorem. Axioms, 11(2), 70. https://doi.org/10.3390/axioms11020070

[19] Sadek, L., & Sami Bataineh, A. (2024). The general Bernstein function: Application to χ-fractional differential equations. Mathematical Methods in the Applied Sciences, 47(7), 6117-6142. https://doi.org/10.1002/mma.9910

[20] Barzegar, N., Mirzaee, F., & Solhi, E. (2025). New Technique Based on Vieta–Lucas Polynomials for Solving Nonlinear Stochastic Itô-Volterra Integral Equation. International Journal of Numerical Modelling: Electronic Networks, Devices and Fields, 38(3), e70044. https://doi.org/10.1002/jnm.70044

[21] Mirzaee, F., Naserifar, S., & Solhi, E. (2024). Meshless Barycentric rational interpolation method for solving nonlinear stochastic fractional integro-differential equations. Iranian Journal of Science, 48(3), 709-733. https://doi.org/10.1007/s40995-024-01621-z

[22] Solhi, E., Mirzaee, F., & Naserifar, S. (2024). Enhanced moving least squares method for solving the stochastic fractional Volterra integro-differential equations of Hammerstein type. Numerical Algorithms, 95(4), 1921-1951. https://doi.org/10.1007/s11075-023-01633-7

[23] Mirzaee, F., Naserifar, S., & Solhi, E. (2023). Accurate and stable numerical method based on the Floater-Hormann interpolation for stochastic Itô-Volterra integral equations. Numerical Algorithms, 94(1), 275-292. https://doi.org/10.1007/s11075-023-01500-5

[24] Solhi, E., Mirzaee, F., & Naserifar, S. (2023). Approximate solution of two dimensional linear and nonlinear stochastic Itô–Volterra integral equations via meshless scheme. Mathematics and Computers in Simulation, 207, 369-387. https://doi.org/10.1016/j.matcom.2023.01.009

[25] Naserifar, S., & Mirzaee, F. (2025). Innovative computational model for variable order fractional Brownian motion and solving stochastic differential equations. Numerical Algorithms, 1-30. https://doi.org/10.1007/s11075-025-02083-z

[26] Dehghan, M., & Abbaszadeh, M. (2019). Error estimate of finite element/finite difference technique for solution of two-dimensional weakly singular integro-partial differential equation with space and time fractional derivatives. Journal of Computational and Applied Mathematics, 356, 314-328. https://doi.org/10.1016/j.cam.2018.12.028

[27] Mirzaee, F., & Alipour, S. (2019). Fractional-order orthogonal Bernstein polynomials for numerical solution of nonlinear fractional partial Volterra integro-differential equations. Mathematical Methods in the Applied Sciences, 42(6), 1870-1893. https://doi.org/10.1002/mma.5481

[28] Sadek, L., Bataineh, A. S., Isik, O. R., Alaoui, H. T., & Hashim, I. (2023). A numerical approach based on Bernstein collocation method: Application to differential Lyapunov and Sylvester matrix equations. Mathematics and Computers in Simulation, 212, 475-488. https://doi.org/10.1016/j.matcom.2023.05.011

[29] Sadek, L., Yüzbaşi, Ş., & Alaoui, H. T. (2024). Two numerical solutions for solving linear and nonlinear systems of differential equations. AApplied and Computational Mathematics, 2024, 23(4), pp. 421–436.

[30] Mercier, A., & Jézéquel, L. (2023). Nonlinear and stochastic analysis of dynamical instabilities based on Chebyshev polynomial properties and applied to a mechanical system with friction. Mechanical Systems and Signal Processing, 189, 110051. https://doi.org/10.1016/j.ymssp.2022.110051

[31] Çenesiz, Y., Keskin, Y., & Kurnaz, A. (2010). The solution of the Bagley-Torvik equation with the generalized Taylor collocation method. Journal of the Franklin institute, 347(2), 452-466. https://doi.org/10.1016/j.jfranklin.2009.10.007

[32] Alzabut, J., Abdeljawad, T., Jarad, F., & Sudsutad, W. (2019). A Gronwall inequality via the generalized proportional fractional derivative with applications. Journal of Inequalities and Applications, 2019(1), 1-12. https://doi.org/10.1186/s13660-019-2052-4.

[33] Boucenna, D., Baleanu, D., Makhlouf, A. B., & Nagy, A. M. (2021). Analysis and numerical solution of the generalized proportional fractional Cauchy problem. Applied Numerical Mathematics, 167, 173-186. https://doi.org/10.1016/j.apnum.2021.04.015

[34] Sharma, V., & Singh, V. K. (2026). Approximation of generalized time fractional derivatives: Error analysis via scale and weight functions. Mathematics and Computers in Simulation. https://doi.org/10.1016/j.matcom.2026.01.027.